

Reverse time shot-geophone migration

Christiaan C. Stolk * *William W. Symes* †, and *Biondo Biondi* ‡

ABSTRACT

Shot-geophone migration, commonly accomplished using wavefield depth extrapolation (“survey sinking”), has a two way reverse time realization as well. The reverse time version permits imaging of overturned reflections, in contrast to the conventional implementation using depth extrapolation (“double square root equation”). However it is implemented, shot-geophone migration differs from other prestack migrations - common offset, common shot or shot profile, common angle... - in the definition of the prestack image volume which it creates. This difference is most clearly seen by identifying shot-geophone migration as the adjoint of an appropriate forward modeling operator. The offset vector in shot-geophone migration need not be horizontal, and this fact can be used to good effect in constructing prestack images of near-vertical or overturned structures. Unlike other prestack migrations, the image property characteristic of correct velocity - focussing of reflection energy at zero offset - holds in strongly refracting media.

INTRODUCTION

The basis of migration velocity analysis is the *semblance principle*: prestack migrated data volumes contain *flat image gathers*, i.e. are at least kinematically independent of the bin or stacking parameter, when the velocity is correct (Yilmaz,...). Migration velocity analysis (as opposed to standard NMO-based velocity analysis) is most urgently needed in areas of strong lateral velocity variation, i.e. “complex” structure such as salt flanks, chalk tectonics, and overthrust geology. However strong refraction implies multiple raypaths connecting source and receiver locations with reflection points, and multiple raypaths in turn imply that the semblance principle is not valid: that is, image gathers are *not* in general flat when the migration velocity close approximates the true propagation velocity.

The failure of the semblance principle in complex structure afflicts all prestack migration techniques based on data binning, i.e. for which each data bin creates an independent

*The Rice Inversion Project, Department of Computational and Applied Mathematics, Rice University, Houston TX 77251-1892 USA, email cstolk@caam.rice.edu.

†The Rice Inversion Project, Department of Computational and Applied Mathematics, Rice University, Houston TX 77251-1892 USA, email symes@caam.rice.edu.

‡Stanford Exploration Project, Department of Geophysics, Stanford University, Stanford CA 94305-2215 USA, email biondo@sep.stanford.edu.

image. This category includes many variants of common shot, common offset and common scattering angle migration - see (Nolan and Symes, 1996; Nolan and Symes, 1997; Xu et al., 2001; Prucha et al., 1999; Stolk, *ress*; Stolk and Symes, 2002). However one well-known form of prestack image formation does *not* migrate image bins independently: this is Claerbout's *survey-sinking migration* (Claerbout, 1985), commonly implemented using the *double square root* ("DSR") equation to extrapolate source and receiver depths. The semblance principle for survey sinking migration is different: rather than being flat in offset, energy is *focussed* at zero offset when the velocity is kinematically correct. This paper refers to this variant of the semblance principle as the *focussing property*.

Note that survey sinking migration is limited to migration velocity model - data combinations in which rays carrying significant energy travel essentially vertically (the "DSR condition", per (Stolk and deHoop, 2001)).

Recently (Stolk and deHoop, 2001) showed that survey sinking does *not* create image artifacts, i.e. that the focussing property holds in media of essentially arbitrary complexity, provided that the DSR condition is valid. Stolk and deHoop also showed that a "Kirchhoff" or diffraction sum implementation is possible, which makes it clear that depth extrapolation *per se* is not the explanation for the good semblance (focussing) property of survey sinking migration. The basis of this ray theoretic analysis is a DSR forward modeling operator, of which the survey-sinking migration operator is the adjoint.

Once one understands survey-sinking migration as the adjoint operator of a shot-geophone model, it is clear that this migration is a special case of a general class of *shot-geophone migration methods*, and that these can be formulated without reference to one-way wavefield extrapolation. The purpose of this paper is to introduce this more general family of migration operators, describe two-way reverse time methods for computing them, and to establish their artifact-free nature. We give a different and somewhat simpler argument than the one in (Stolk and deHoop, 2001) for the absence of kinematic artifacts. In contrast to (Claerbout, 1985; Stolk and deHoop, 2001), our formulation and analysis accomodates *non-horizontal offset*, and we explain the importance of this generalization for imaging near-vertical or overturned structure. Imaging of reflectors at arbitrary angle of dip requires that the dip vector not be parallel to the direction of offset - otherwise the focussing property is lost, for example in attempting to image a vertical reflector using only horizontal offsets in shot-geophone migration. We illustrate this phenomenon with simple examples, and explain it via ray theory.

When the DSR condition holds, our analysis provides an alternate (and, we think, simpler) justification for the no-artifacts result of (Stolk and deHoop, 2001) than does that paper, as well as an alternate computational approach. For the general (non-DSR) case we propose a method for imaging all dips simultaneously by combining two or more depth offset directions, with appropriate dip filtering. In this case, the focussing property cannot in general be guaranteed in the simple form for which it holds when the DSR condition is satisfied. Instead, we show that image volume energy is localized (i) at zero offset, and (ii) possibly outside a corridor around zero offset. We relate the width of the corridor to properties of the ray fields, which are necessary for a final stacked image at

correct velocity to faithfully render the reflectors in the subsurface (traveltime injectivity condition, no scattering over π).

The papers (Biondi and Shan, 2002; Biondi and Symes, 2003) introduce essentially the same family of reverse time algorithms, and discuss some of their properties. In particular these papers shows that shot-geophone reverse time migration retains the property which has led in the past to interest in reverse time migration (Whitmore, 1983; Chang and McMechan, 1994; Yoon et al., 2003): it images reflectors which are invisible to depth extrapolation migration due to overturned raypaths. The approach to imaging all dips proposed in (Biondi and Symes, 2003) produces a single angle domain volume, rather than the three offset domain volumes (one for each coordinate axis) proposed here. The input to the angle domain image construction is essentially the three image volumes defined in this paper, however, and the two approaches are very closely related.

TWO WAY SHOT-GEOPHONE MIGRATION

This section introduces shot-geophone migration as the adjoint of a shot-geophone modeling operator, with a completely general offset vector. In an appendix we show how Claerbout's survey sinking migration arises as a special case.

We assume that sources and receivers lie on the same depth plane, and adjust the depth axis so that the source-receiver plane is $z = 0$. This restriction is can be removed at the cost of more complicated notation (and numerics): it is not essential.

While the examples to be presented later are all 2D, the construction is not: in the following \mathbf{x} (and other bold face letters) will denote either two- or three-dimensional vectors. Source locations are \mathbf{x}_s , receiver locations are \mathbf{x}_r . Note in particular that nothing about the formulation of the migration method *requires* that data be given on the full surface $z = 0$.

Single scattering

The causal acoustic Green's function $G(\mathbf{x}, t; \mathbf{x}_s)$ for a point source at $\mathbf{x} = \mathbf{x}_s$ is the solution of

$$\frac{1}{v^2(\mathbf{x})} \frac{\partial^2 G}{\partial t^2}(\mathbf{x}, t; \mathbf{x}_s) - \nabla_{\mathbf{x}}^2 G(\mathbf{x}, t; \mathbf{x}_s) = \delta(\mathbf{x} - \mathbf{x}_s) \delta(t) \quad (1)$$

with $G = 0, t < 0$.

In common with all other migration methods, shot-geophone migration is based on the Born or single scattering approximation. Denote by $r(\mathbf{x}) = \delta v(\mathbf{x})/v(\mathbf{x})$ a relative perturbation of the velocity field. Then linearization of the wave equation yields for the corresponding perturbation of the Green's function

$$\frac{1}{v^2(\mathbf{x})} \frac{\partial^2 \delta G}{\partial t^2}(\mathbf{x}, t; \mathbf{x}_s) - \nabla_{\mathbf{x}}^2 \delta G(\mathbf{x}, t; \mathbf{x}_s) = \frac{2r(\mathbf{x})}{v^2(\mathbf{x})} \frac{\partial^2}{\partial t^2} G(\mathbf{x}, t; \mathbf{x}_s) \quad (2)$$

whose solution has the integral representation at the source and receiver points $\mathbf{x}_r, \mathbf{x}_s$

$$\delta G(\mathbf{x}_r, t; \mathbf{x}_s) = \frac{\partial^2}{\partial t^2} \int dx \int dh \int d\tau \frac{2r(\mathbf{x})}{v^2(\mathbf{x})} G(\mathbf{x}, t - \tau; \mathbf{x}_r) G(\mathbf{x}, \tau; \mathbf{x}_s) \quad (3)$$

The singly scattered field is the time convolution of δG with a source wavelet (or the space-time convolution with a radiation pattern operator, for more complex sources). Since the principal concern of this paper is kinematic relationships between data and image, we will ignore the filtering by the source signature (i.e. replace it with a delta function). This effective replacement of the source by an impulse does not seem to invalidate the predictions of the theory, though the matter is certainly worthy of more study.

Thus the Born modeling operator $F[v]$ is

$$F[v]r(\mathbf{x}_r, t; \mathbf{x}_s) = \delta G(\mathbf{x}_r, t; \mathbf{x}_s)$$

Prestack shot profile modeling results from replacing $2r(\mathbf{x})/v^2(\mathbf{x})$ with $R(\mathbf{x}, \mathbf{x}_s)$, i.e. permitting reflectivity to be defined differently for each shot. Examination of equation (2) shows that each shot is then modeled independently of every other. The adjoint of the shot profile modeling operator is shot profile migration; since Born modeling is just shot profile modeling with $R(\mathbf{x}, \mathbf{x}_s) = 2r(\mathbf{x})/v^2(\mathbf{x})$, Born migration is shot profile migration followed by the adjoint of the ‘‘spray’’ mapping $r(\mathbf{x}) \mapsto R(\mathbf{x}, \mathbf{x}_s) = 2r(\mathbf{x})/v^2(\mathbf{x})$, which is the stack. The other standard prestack migrations via data binning have similar relationships to Born migration.

Shot-geophone modeling and migration in midpoint-offset coordinates

Shot-geophone modeling results from a different generalization of reflectivity: replace $2r(\mathbf{x})/v^2(\mathbf{x})$ by $R(\mathbf{x}, \mathbf{h})$ where \mathbf{h} is the depth (half)offset mentioned in the introduction. The coordinate \mathbf{x} plays the role of midpoint.

Remark: If the velocity is constant, at least locally in a region to be imaged, it is possible to interpret the midpoint \mathbf{x} as an image point (Biondi and Symes, 2003). In general this is not possible, and only the offset coordinate \mathbf{h} has direct physical significance.

Replace the Born scattering field δG by the shot-geophone field $\delta \bar{G}$, defined by equation (3) by

$$\delta \bar{G}(\mathbf{x}_r, t; \mathbf{x}_s) = \frac{\partial^2}{\partial t^2} \int dx \int dh \int d\tau R(\mathbf{x}, \mathbf{h}) G(\mathbf{x} + \mathbf{h}, t - \tau; \mathbf{x}_r) G(\mathbf{x} - \mathbf{h}, \tau; \mathbf{x}_s) \quad (4)$$

It is also possible to view $\delta \bar{G}$ as the value at $\mathbf{y} = \mathbf{x}_r$ of a modified shot-profile field $u(\mathbf{y}, t; \mathbf{x}_s)$ which solves

$$\frac{1}{v^2(\mathbf{y})} \frac{\partial^2 u}{\partial t^2}(\mathbf{y}, t; \mathbf{x}_s) - \nabla_{\mathbf{y}}^2 u(\mathbf{y}, t; \mathbf{x}_s) = \int dh R(\mathbf{y} - \mathbf{h}, \mathbf{h}) \frac{\partial^2}{\partial t^2} G(\mathbf{y} - 2\mathbf{h}, t; \mathbf{x}_s) \quad (5)$$

The shot-geophone modeling operator $\bar{F}[v]$ is given by

$$\bar{F}[v]R(\mathbf{x}_r, t; \mathbf{x}_s) = \delta \bar{G}(\mathbf{x}_r, t; \mathbf{x}_s)$$

The field $\delta \bar{G}(\mathbf{x}, t; \mathbf{x}_s)$ is identical to $\delta G(\mathbf{x}, t; \mathbf{x}_s)$ when

$$R(\mathbf{x}, \mathbf{h}) = \frac{2r(\mathbf{x})}{v^2(\mathbf{x})} \delta(\mathbf{h})$$

i.e. when the generalized reflectivity is concentrated at offset zero. Therefore Born modeling is shot-geophone modeling following the mapping

$$r(\mathbf{x}) \mapsto \frac{2r(\mathbf{x})}{v^2(\mathbf{x})}\delta(\mathbf{h}) \quad (6)$$

Born migration is then shot-geophone migration followed by the adjoint of the mapping defined in equation (6), i.e. which is

$$R(\mathbf{x}, \mathbf{h}) \mapsto \frac{2R(\mathbf{x}, 0)}{v^2(\mathbf{x})} \quad (7)$$

i.e. shot-geophone migration followed by extraction off the zero offset section.

The shot-geophone migration operator is the adjoint of the shot-geophone modeling operator. Its reverse time implementation is a minor variation on the usual implementation of reverse time migration (the ‘‘adjoint state method’’, see eg. (Tarantola, 1987; Whitmore, 1983; Lailly, 1983)). We give a derivation in Appendix A, for the sake of completeness. The result is

$$\bar{F}^*[v]d(\mathbf{x}, \mathbf{h}) = - \int dx_s \int_0^T dt \left(\frac{\partial q}{\partial t} \nabla^2 G \right) (\mathbf{x} - 2\mathbf{h}, t; \mathbf{x}_s) \quad (8)$$

where the *adjoint state* or backpropagated field $q(\mathbf{x}, t; \mathbf{x}_s)$ satisfies $q \equiv 0$, $t \geq T$ and

$$\left(\frac{1}{v(\mathbf{x})^2} \frac{\partial^2}{\partial t^2} - \nabla_{\mathbf{x}}^2 \right) q(\mathbf{x}, t; \mathbf{x}_s) = \int dx_r d(\mathbf{x}_r, t; \mathbf{x}_s) \delta(\mathbf{x} - \mathbf{x}_r) \quad (9)$$

Remark: Note that the backpropagated field is *not* in general the physical scattered field, time-reversed. It is a mathematical convenience which permits a simple computation of the adjoint, with no immediate physical significance. Discretization of the wave equation for the scattered field (2), eg. by finite differences, gives a linear system, written implicitly as a recursion. The calculation specified by equations (8,9) is the continuous limit of the transposed system, again written implicitly as a recursion.

The migration operator defined by equations (8,9) is very similar to the usual prestack reverse time migration operator:

1. The adjoint state field q is *exactly* the same as the usual adjoint state field which appears in two-way reverse time migration, i.e. the solution of the problem (9), and is computed independently for each shot;
2. The Green’s function $G(\mathbf{x}, t; \mathbf{x}_s)$ is *exactly* the same reference field used in shot profile two way reverse time migration, i.e. the solution of the problem (1), and can also be computed shot-by-shot;
3. The imaging condition (8) is *exactly* the same as the usual two-way reverse time shot profile imaging condition when $\mathbf{h} = 0$; the latter is the reverse time version of Claerbout’s survey-sinking imaging condition (Claerbout, 1985).

4. Therefore the only real difference with standard two way reverse time migration comes in the \mathbf{h} dependence in (8), which implies a loop over \mathbf{h} . Note that this does not require the solution of any new PDEs: it simply inserts a new loop in the computation of the adjoint image (migration output), over \mathbf{h} . Thus the image can still be accumulated in a loop over shots of independent, shot-by-shot computations, exactly as is done in standard reverse time migration. The additional computational burden of the \mathbf{h} loop depends on the sampling and range of \mathbf{h} .

Shot-geophone modeling and migration in source-receiver coordinates

It turns out to be convenient to introduce a more symmetrical representation of shot-geophone modeling, which we dub the *source-receiver representation*.

Define coordinates $\mathbf{y}_s = \mathbf{x} - \mathbf{h}$, $\mathbf{y}_r = \mathbf{x} + \mathbf{h}$; these will turn out to be coordinates along rays from source and receiver respectively. Define the *source-receiver reflectivity* \bar{R} by

$$\bar{R}(\mathbf{y}_s, \mathbf{y}_r) = R\left(\frac{\mathbf{y}_s + \mathbf{y}_r}{2}, \frac{\mathbf{y}_r - \mathbf{y}_s}{2}\right), \text{ i.e. } \bar{R}(\mathbf{x} - \mathbf{h}, \mathbf{x} + \mathbf{h}) = R(\mathbf{x}, \mathbf{h})$$

Then change integration variables in equation (4)

$$\bar{F}[v]\bar{R}(\mathbf{x}_r, t; \mathbf{x}_s) = \frac{1}{2} \frac{\partial^2}{\partial t^2} \int dy_s \int dy_r \int d\tau \bar{R}(\mathbf{y}_s, \mathbf{y}_r) G(\mathbf{y}_r, t - \tau; \mathbf{x}_r) G(\mathbf{y}_s, \tau; \mathbf{x}_s) \quad (10)$$

It follows that

$$F[v]R(\mathbf{x}_r, t; \mathbf{x}_s) = \bar{F}[v]\bar{R}(\mathbf{x}_r, t; \mathbf{x}_s) = u(\mathbf{x}_r, t; \mathbf{x}_s)$$

where u solves both

$$\frac{1}{v^2(\mathbf{x})} \frac{\partial^2 u}{\partial t^2}(\mathbf{x}, t; \mathbf{x}_s) - \nabla_{\mathbf{x}}^2 u(\mathbf{x}, t; \mathbf{x}_s) = \int dy_s \bar{R}(\mathbf{y}_s, \mathbf{x}) \frac{\partial^2}{\partial t^2} G(\mathbf{y}_s, t; \mathbf{x}_s) \quad (11)$$

and

$$\frac{1}{v^2(\mathbf{x})} \frac{\partial^2 u}{\partial t^2}(\mathbf{x}_r, t; \mathbf{x}) - \nabla_{\mathbf{x}}^2 u(\mathbf{x}_r, t; \mathbf{x}) = \int dy_r \bar{R}(\mathbf{x}, \mathbf{y}_r) \frac{\partial^2}{\partial t^2} G(\mathbf{y}_r, t; \mathbf{x}_r) \quad (12)$$

The source-receiver representation of shot-geophone migration is

$$\bar{F}[v]^* d(\mathbf{y}_s, \mathbf{y}_r) = \int dx_s \int dt q(\mathbf{y}_r, t; \mathbf{x}_s) \frac{\partial^2}{\partial t^2} G(\mathbf{y}_s, t; \mathbf{x}_s) \quad (13)$$

in which q is the backpropagated field described in the last subsection (solution of equation (9)). Note that the imaging condition (13) collapses to the usual imaging condition when \mathbf{y}_s and \mathbf{y}_r coincide with an image point (zero offset).

Remark: The source-receiver representation is important for the kinematic analysis to follow. However the midpoint-offset representation is more convenient for computation.

Kirchhoff representation of shot-geophone migration

An integral or ‘‘Kirchhoff’’ representation of the shot-geophone migration operator is also possible. We mention this here to emphasize that the computational representation of the shot-geophone migrated field is not the determinant of its favorable kinematic properties: two way reverse time, Kirchhoff, and depth extrapolation computations will yield equivalent migrations, within the domain of validity of each. The Kirchhoff representation described here is in principle kinematically equivalent to two-way reverse time computation, as described in the previous subsection. Depth extrapolation computations have a more restricted domain of validity.

Application of standard high frequency asymptotics and stationary phase arguments to the integral representation of the shot-geophone field (3) gives

$$F[v]R(\mathbf{x}_r, t; \mathbf{x}_s) = \frac{\partial^2}{\partial t^2} \sum_{i,j} \int \int dx dh A^{(i,j)}(\mathbf{x}, \mathbf{h}, \mathbf{x}_s, \mathbf{x}_r) \delta(t - T^{(i,j)}(\mathbf{x}, \mathbf{h}, \mathbf{x}_s, \mathbf{x}_r)) R(\mathbf{x}, \mathbf{h}) \quad (14)$$

(see REFS) in which $T^{(i,j)}(\mathbf{x}, \mathbf{h}, \mathbf{x}_s, \mathbf{x}_r)$ is the sum of the i th branch of the (one-way) traveltimes from the source point \mathbf{x}_s to the source-ray scattering point $\mathbf{x} - \mathbf{h}$, and the j th branch of the traveltimes from the receiver-ray scattering point $\mathbf{x} + \mathbf{h}$ to the receiver point \mathbf{x}_r , and $A^{(i,j)}(\dots)$ is an amplitude involving spreading factors, velocity, etc. The Kirchhoff shot-geophone migration formula is then

$$F^*[v]d(\mathbf{x}, \mathbf{h}) \simeq \int \int dx_s dx_r \sum_{i,j} A^{(i,j)}(\mathbf{x}, \mathbf{h}, \mathbf{x}_s, \mathbf{x}_r) \frac{\partial^2 d}{\partial t^2}(\mathbf{x}_s, \mathbf{x}_r, T^{(i,j)}(\mathbf{x}, \mathbf{h}, \mathbf{x}_s, \mathbf{x}_r)) \quad (15)$$

These formulas were derived in a different way in (Stolk and deHoop, 2001) for the special case $h_3 = 0$, i.e. horizontal depth-offset, and used to analyze the kinematics of shot-geophone migration, to which we now turn.

KINEMATICS OF SHOT-GEOPHONE MIGRATION

An event in the data is characterized by its (3D) moveout: locally, by a moveout equation $t = T(\mathbf{x}_s, \mathbf{x}_r)$, and infinitesimally by the source and receiver slownesses

$$\mathbf{p}_s = \nabla_{\mathbf{x}_s} T, \quad \mathbf{p}_r = \nabla_{\mathbf{x}_r} T$$

Significant energy with this moveout implies that locally near $(\mathbf{x}_s, \mathbf{x}_r, t)$ the data contains a plane wave component with wavenumber $(\omega \mathbf{p}_s, \omega \mathbf{p}_r, \omega)$. These coordinates (position, wavenumber) give the phase space representation of the event.

Note that for incomplete coverage, eg. marine streamer geometry, an event in the data will not determine its (3D) moveout uniquely. For example, in (idealized) marine streamer geometry, with the streamers oriented along the x axis, the y component of \mathbf{p}_r is not determined by the data. In the discussion to follow, \mathbf{p}_s and \mathbf{p}_r are assumed to be *compatible* with a data event.

Likewise, a reflector (in the source-receiver representation) at $(\mathbf{y}_s, \mathbf{y}_r)$ with wavenumber $(\mathbf{k}_s, \mathbf{k}_r)$ is characterized in (image volume) phase space by these coordinates.

The kinematical description of shot-geophone migration relates the phase space coordinates of events and reflectors. An event with phase space representation $(\mathbf{x}_s, \mathbf{x}_r, t_{sr}, \omega \mathbf{p}_s, \omega \mathbf{p}_r, \omega)$ is the result of a reflector with (double reflector) phase space representation $(\mathbf{y}_s, \mathbf{y}_r, \mathbf{k}_s, \mathbf{k}_r)$ exactly when

- there is a ray $(\mathbf{X}_s, \mathbf{P}_s)$ leaving the source point $\mathbf{X}_s(0) = \mathbf{x}_s$ at time $t = 0$ with ray parameter $\mathbf{P}_s(0) = \mathbf{p}_s$, and arriving at $\mathbf{X}_s(t_s) = \mathbf{y}_s$ at $t = t_s$ with ray parameter $\mathbf{P}_s(t_s) = -\mathbf{k}_s/\omega$;
- there is a ray $(\mathbf{X}_r, \mathbf{P}_r)$ leaving $\mathbf{X}_r(t_s) = \mathbf{y}_r$ at $t = t_s$ with ray parameter $\mathbf{P}_r(t_s) = \mathbf{k}_r/\omega$ and arriving at the receiver point $\mathbf{X}_r(t_{sr}) = \mathbf{x}_s$ at time $t = t_{sr} = t_s + t_r$ with ray parameter $\mathbf{P}_r(t_{sr}) = \mathbf{p}_r$.

This situation is illustrated in Figure .

A derivation of this relation is given in Appendix B.

Note that since $\mathbf{P}_s, \mathbf{P}_r$ are ray slowness vectors, there is necessarily a length relation between $\mathbf{k}_s, \mathbf{k}_r$: namely,

$$\frac{1}{v(\mathbf{y}_s)} = \|\mathbf{P}_s(t_s)\| = \frac{\|\mathbf{k}_s\|}{|\omega|}$$

$$\frac{1}{v(\mathbf{y}_r)} = \|\mathbf{P}_r(t_r)\| = \frac{\|\mathbf{k}_r\|}{|\omega|}$$

whence

$$\frac{\|\mathbf{k}_r\|}{\|\mathbf{k}_s\|} = \frac{v(\mathbf{y}_s)}{v(\mathbf{y}_r)} \quad (16)$$

The kinematics of shot-geophone migration are somewhat strange, so it is reassuring to see that for physical reflectors (i.e. $\bar{R}(\mathbf{y}_s, \mathbf{y}_r) = r(\mathbf{x})\delta(\mathbf{h})$) the relation just explained becomes the familiar one of reflection from a reflecting element according to Snell's law. A quick calculation shows that such a physical \bar{R} has a significant local plane wave component near $(\mathbf{y}_s, \mathbf{y}_r)$ with wavenumber $(\mathbf{k}_s, \mathbf{k}_r)$ only if $\mathbf{y}_s = \mathbf{y}_r = \mathbf{x}$ and r has a significant local plane wave component near \mathbf{x} with wavenumber $\mathbf{k}_x = \mathbf{k}_s + \mathbf{k}_r$. From equation (16), \mathbf{k}_s and \mathbf{k}_r have the same length, therefore their sum \mathbf{k}_x is also their bisector, which establishes Snell's law. Thus a single (physical) reflector at \mathbf{x} with wavenumber ξ gives rise to a reflected event at frequency ω exactly when the rays $(\mathbf{X}_s, \mathbf{P}_s)$ and $(\mathbf{X}_r, \mathbf{P}_r)$ meet at \mathbf{x} at time t_s , and the reflector dip $\mathbf{k}_x = \omega(\mathbf{P}_r(t_s) - \mathbf{P}_s(t_s))$, which is the usual kinematics of single scattering. See Figure .

It is now possible to answer the question: in the shot-geophone model, to what extent does a data event determine the corresponding reflector? The rules derived above show that the reflection point $(\mathbf{y}_s, \mathbf{y}_r)$ must lie on the Cartesian product of two rays, $(\mathbf{X}_s, \mathbf{P}_s)$ and $(\mathbf{X}_r, \mathbf{P}_r)$, consistent with the event, and the total time is also determined. If the coverage is complete, so that the event uniquely determines the source and receiver rays,

then the source-receiver representation of the source-receiver reflector must lie along this uniquely determined ray pair. This fact contrasts dramatically with the imaging ambiguities demonstrated in (Nolan and Symes, 1996; Nolan and Symes, 1997; Xu et al., 2001; Prucha et al., 1999; Stolk, res; Stolk and Symes, 2002) for all forms of prestack depth migration based on data binning. Even when coverage is complete, in these other forms of prestack migration strong refraction leads to multiple ray pairs connecting data events and reflectors, whence ambiguous imaging of a single event in more than one location within the prestack image volume.

Nonetheless reflector location is still not uniquely determined by shot-geophone migration as defined above, for two reasons:

- Only the total travelttime is specified by the event! Thus if $\mathbf{y}_s = \mathbf{X}_s(t_s)$, $\mathbf{y}_r = \mathbf{X}_r(t_s)$ are related as described above to the event determining the ray pair, so is $\mathbf{y}'_s = \mathbf{X}_s(t'_s)$, $\mathbf{y}'_r = \mathbf{X}_r(t'_s)$ with $t_s + t_r = t'_s + t'_r = t_{sr}$. See Figure .
- Incomplete coverage may prevent the event from determining its 3D moveout, as mentioned above, and therefore a family of ray pairs, rather than a unique ray pair, corresponds to the event.

KINEMATICS WITH RESTRICTED OFFSETS

One way to view the remaining imaging ambiguity in shot-geophone migration as defined so far is to recognize that the image point coordinates $(\mathbf{y}_s, \mathbf{y}_r)$ (or (\mathbf{x}, \mathbf{h})) are six-dimensional (in 3D), whereas the data depends on only five coordinates $(\mathbf{x}_r, t, \mathbf{x}_s)$ (at most). Formally, restricting one of the coordinates of the image point to be zero would at least make the variable counts equal, so that unambiguous imaging would at least be conceivable. Since physical reflectivities are concentrated at zero (vector) offset, it is natural to restrict one of the offset coordinates to be zero.

Imaging conditions with restricted offsets

In 3D, there are three possibilities, in which $R(\mathbf{x}, \mathbf{h})$ takes one of the three forms

$$R_x(\mathbf{x}, h_y, h_z)\delta(h_x), \quad R_y(\mathbf{x}, h_x, h_z)\delta(h_y), \quad R_z(\mathbf{x}, h_x, h_y)\delta(h_z)$$

leading to three restricted modeling operators:

$$\begin{aligned} \bar{F}_x[v]R_x(\mathbf{x}_r, t; \mathbf{x}_s) &= \frac{\partial^2}{\partial t^2} \int dx \int dh_y \int dh_z \int d\tau \\ R_x(\mathbf{x}, h_y, h_z)G(\mathbf{x} + (0, h_y, h_z), t - \tau; \mathbf{x}_r)G(\mathbf{x} - (0, h_y, h_z), \tau; \mathbf{x}_s) \end{aligned} \quad (17)$$

$$\begin{aligned} \bar{F}_y[v]R_y(\mathbf{x}_r, t; \mathbf{x}_s) &= \frac{\partial^2}{\partial t^2} \int dx \int dh_x \int dh_z \int d\tau \\ R_x(\mathbf{x}, h_x, h_z)G(\mathbf{x} + (h_x, 0, h_z), t - \tau; \mathbf{x}_r)G(\mathbf{x} - (h_x, 0, h_z), \tau; \mathbf{x}_s) \end{aligned} \quad (18)$$

$$\begin{aligned} \bar{F}_z[v]R_z(\mathbf{x}_r, t; \mathbf{x}_s) &= \frac{\partial^2}{\partial t^2} \int dx \int dh_x \int dh_y \int d\tau \\ R_x(\mathbf{x}, h_x, h_y)G(\mathbf{x} + (h_x, h_y, 0), t - \tau; \mathbf{x}_r)G(\mathbf{x} - (h_x, h_y, 0), \tau; \mathbf{x}_s) \end{aligned} \quad (19)$$

The kinematics of these restricted operators follows directly from that of the unrestricted operator, developed in the preceding section. Denote $\mathbf{y}_s = (x_s, y_s, z_s)$, $\mathbf{k}_s = (k_{s,x}, k_{s,y}, k_{s,z})$ etc.

For restricted x offset,

$$\bar{R}(\mathbf{y}_s, \mathbf{y}_r) = \bar{R}_x \left(\frac{x_s + x_r}{2}, y_s, y_r, z_s, z_r \right) \delta(x_s - x_r)$$

Fourier transformation shows that \bar{R} has a significant plane wave component with wavenumber $(\mathbf{k}_s, \mathbf{k}_r)$ precisely when \bar{R}_x has a significant plane wave component with wavenumber $(k_{s,x} + k_{r,x}, k_{s,y}, k_{s,z}, k_{r,y}, k_{r,z})$. Thus a ray pair $(\mathbf{X}_s, \mathbf{P}_s)$, $(\mathbf{X}_r, \mathbf{P}_r)$ compatible with a data event with phase space coordinates $(\mathbf{x}_r, \mathbf{x}_s, t_{sr}, \omega\mathbf{p}_s, \omega\mathbf{p}_r, \omega)$ images at a point $(x, y_s, y_r, z_s, z_r, k_x, k_{s,y}, k_{s,z}, k_{r,y}, k_{r,z})$ provided that for $0 \leq t_s \leq t_{sr}$, $X_{s,x}(t_s) = X_{r,x}(t_s) = x$, $X_{s,y}(t_s) = y_s$, $X_{r,y}(t_s) = y_r$, $X_{s,z}(t_s) = z_s$, $X_{r,z}(t_s) = z_r$, $P_{r,x}(t_s) - P_{s,x}(t_s) = k_s/\omega$, $P_{s,y}(t_s) = k_{s,y}/\omega$, etc.

Similarly, for restricted y offset,

$$\bar{R}(\mathbf{y}_s, \mathbf{y}_r) = \bar{R}_y \left(x_s, x_r, \frac{y_s + y_r}{2}, z_s, z_r \right) \delta(y_s - y_r)$$

and the imaging conditions are $X_{s,y}(t_s) = X_{r,y}(t_s) = y$, $P_{r,y}(t_s) - P_{s,y}(t_s) = k_s/\omega$, $X_{s,x}(t_s) = x_s$, $P_{s,x}(t_s) = k_{s,x}/\omega$, etc. at image phase space point $(x_s, x_r, y, z_s, z_r, k_{s,x}, k_{r,x}, k_y, k_{s,z}, k_{r,z})$.

For restricted z offset,

$$\bar{R}(\mathbf{y}_s, \mathbf{y}_r) = \bar{R}_z \left(x_s, x_r, y_s, y_r, \frac{z_s + z_r}{2} \right) \delta(z_s - z_r)$$

and the imaging conditions are $X_{s,z}(t_s) = X_{r,z}(t_s) = z$, $P_{r,z}(t_s) - P_{s,z}(t_s) = k_z/\omega$, $X_{s,x}(t_s) = x_s$, $P_{s,x}(t_s) = k_{s,x}/\omega$, etc. at image phase space point $(x_s, x_r, y_s, y_r, z, k_{s,x}, k_{r,x}, k_{s,y}, k_{r,y}, k_z)$.

Horizontal offset and the DSR condition

As explained in Appendix C, Claerbout's survey sinking migration is kinematically equivalent to shot-geophone migration as defined here, under two assumptions:

- offsets are restricted to horizontal ($h_z = 0$);
- rays (either source or receiver) carrying significant energy do not turn, i.e. $P_{s,z} > 0, P_{r,z} < 0$ throughout the propagation.

We call the second condition the ‘‘Double Square Root’’, or ‘‘DSR’’, condition, for reasons explained in Appendix C.

Claim: Under these restrictions, the imaging operator \bar{F}_z can image a ray pair at precisely one location in image volume phase space. When the velocity is correct, the image energy is therefore concentrated at zero offset.

To see this, note that the condition $X_{s,z}(t_s) = X_{r,z}(t_s)$ can only be satisfied at one value of t_s . The depth is increasing along the source ray, and decreasing along the receiver ray - otherwise put, depth is increasing along both rays, if you traverse the receiver ray *backwards*. Therefore depth can be used to parametrize the rays. Time is increasing from zero along the source ray, and decreasing from t_{sr} along the receiver ray (traversed backwards), viewed as a function of depth. Thus the two times can be equal (to t_s) at exactly one point.

Since the scattering time t_s is uniquely determined, so are all the other phase space coordinates of the rays, hence of the reflector location in phase space, through the conditions for \bar{F}_z imaging laid down in the last section.

If furthermore coverage is complete, whence the data event uniquely determines the rays, then it follows that a data event is imaged at precisely one location. This is the result established in (Stolk and deHoop, 2001), for which we have now given a different (and more elementary) proof.

Remark: Note that the DSR assumption precludes the imaging of near- or post-vertical reflectors.

We present a 2D synthetic example which emphasizes the dramatic contrast, revealed by the Stolk-deHoop theorem, between the behaviour of shot-geophone migration and other forms of prestack migration. This example is used in (Stolk, res; Stolk and Symes, 2002) to show that common offset and Kirchhoff common scattering angle migration generally produce strong kinematic artifacts in strongly refracting velocity models. The velocity model consists of a slow Gaussian lens embedded in a constant background. As shown in Figure , this model is strongly refracting - it produces triplications in rayfields shot from surface points - while still obeying the DSR condition, for the offsets used in the example. Below the lens, at a depth of 2 km, we placed a flat reflector. We synthesized data using a (4, 10, 20, 40) zero phase bandpass filter as (isotropic) source wavelet and a finite difference scheme with adequate sampling. A typical shot gather (Figure) shows the complex pattern of reflections from the flat reflector propagated through the lens.

We migrated this data using the adjoint of the \bar{F}_z modeling operator (equation (19)). The adjoint state method for this computation amounts to the 2D version of equations (8, 9) with $h_z = 0$. Inspection of image gathers ((z, h) slices through the (x, z, h) image volume at various x) show that image energy is focussed at zero offset and at the correct reflector location (depth), as predicted by the theory (Figure ??).

Contrast this behaviour with that of Kirchhoff common offset and common scattering angle migration, Figures , reproduced from (Stolk and Symes, 2002). For these prestack migration methods, defined by surface binning of the data, image gathers should be flat when correct migration velocity is used (as opposed to focussed at one horizontal location, as for shot-geophone migration). Instead, numerous highly energetic non-flat events contaminate the gathers. Missing rays are not the cause: all arrivals are used in

these computations, with correct phase shifts and amplitudes in the imaging formulae. In fact, these events are kinematic in nature: that is, they cannot be removed by more sophisticated signal processing, but are intrinsic to the ray geometry of these migration methods.

Remark: Note that Kirchhoff common scattering angle migration, as used to produce the gather displayed in Figure , is quite different from the angle domain migration proposed in (Prucha et al., 1999; Sava and Fomel, 2003; Biondi and Symes, 2003). The former uses an implicit surface-oriented phase space binning of the data, whereas the latter amounts to a Radon transform of the shot-geophone migration output in depth and offset (or is closely related to this transform). The focussing property of shot-geophone migration, just illustrated, implies that angle domain migration also produces artifact-free image gathers, at least when the DSR condition holds. Figure ?? illustrates this contention.

Combining horizontal and vertical offsets: the Traveltime Injectivity Condition

The DSR assumption will not hold, or permit adequate imaging, in complex lithologic environments with substantial lateral and vertical velocity variation, vertical or overhanging reflectors, etc. However, two other conditions, both necessary in general for imaging given correct velocity, are also sufficient to ensure that the energy in a *properly filtered* source-receiver restricted offset image volumes is concentrated (i) at zero offset, and possibly (ii) at offsets greater than a minimum which depends on various characteristics of the velocity through its ray geometry. That is, in absence of the DSR restriction, energy may appear at nonzero offsets, even with correct velocity, but not within a corridor about zero offset, except at zero offset.

This section explains the physical and geometric significance of these conditions, and the necessity of filtering. Mathematical details appear in Appendix D.

The first of these two conditions is the “no scattering over π ” condition identified already in (Rakesh, 1988) as essential to accurate migration. That is, no energy along direct rays connecting source to receiver can appear in the data submitted to migration. We quantify this condition by demanding that the scattering angle for all ray pairs involved in image construction be less than a maximum angle, which is less than π . This “maximum scattering angle” or MSA condition can in principle be enforced by ray-tracing and selective muting and Radon filtering.

The second condition is the *Traveltime Injectivity Condition* or TIC (tenKroode et al., 1998; Nolan and Symes, 1997). This condition is in general necessary for artifact-free postmigration stacks - i.e. absence of mispositioned reflectors, not in the prestack image volume but in the final stacked image. TIC mandates that *along any pair of rays, at most one point of intersection exists with a given traveltime*. Clearly TIC is also implied by the DSR condition, so TIC generalizes DSR. It is also clear that TIC can be violated - see the cited references for examples.

Under some circumstances standard migration operators (i.e. adjoints of linearized modeling operators) may produce artifact-free images even when TIC is violated - see

(Stolk, 2000) for a discussion of this point. However in general TIC is necessary for artifact-free imaging. A quantitative form of TIC, with a specific estimate of distance vs. time along imaging ray pairs, is explained in Appendix D.

It is less clear how TIC may be enforced for the data submitted to migration. The present results, like those of (tenKroode et al., 1998), simply presume that (the quantitative form of) TIC holds.

As explained earlier, a simple variable count suggests that unambiguous images can only be accomplished by restricting the offset to planes (or lines, for 2D shot-geophone migration). However, without the DSR hypothesis, it is easy to see that the horizontal offset imaging operator, \bar{F}_z , cannot have the focussing property, i.e. focus energy at zero offset for correct velocity.

Figures ?? and ?? show why this is so. Both figures are meant to cartoon imaging at correct velocity, which for convenience is assumed constant near the image point (hence the locally straight rays). In Figure ??, two rays image an event at their intersection on a reflector with nonzero z component of dip. Note that as one moves away from the image point, keeping the total time along the two rays the same, the difference in z components of the ray locations unavoidably grows, so that these (unrestricted) source-receiver image points do not appear in the horizontal offset operator output. That is, only the zero offset image survives restriction to horizontal offset. On the other hand, Figure ?? shows an image point on a vertical reflector; clearly one can move away from the image point, maintaining the same total time, in such a way that these other unrestricted image points have the same z components hence survive the restriction to horizontal offset. Obviously in this case the output of \bar{F}_z will have energy at all offsets sufficiently close to zero, and the focussing property is lost.

Note that the absence of nonzero offset image energy suggested by Figure ?? is a *local* phenomenon. That is, the rays may curve in such a way that points may appear with the same total travel time and z coordinates, sufficiently far away from the physical scattering point - Figure ?? cartoons this situation. The time difference cannot be close to zero, however. As shown in Appendix D, together with TIC and MSA this minimum time difference implies that the offset of any image energy at nonzero offset also exceeds a minimum.

These are not idle speculations: examples presented in (Biondi and Symes, 2003) demonstrate the “smearing” of image gathers in horizontal offset shot-geophone migration (\bar{F}_z^*) as reflector dip approaches horizontal. The inescapable conclusion is that horizontal offset shot-geophone migration cannot image (near) vertical reflectors without degrading the focussing property characteristic of correct velocity. Precisely analogous reasoning shows that x- and y-axis vertical offset shot-geophone migration (\bar{F}_x^* , \bar{F}_y^*) cannot image dips perpendicular to the x-axis and y-axis respectively without smearing in the restricted offset.

On the other hand, any particular dip is well-imaged by at least one of these operators, with focussing at zero offset at least locally, as argued above in the horizontal offset case. The paper (Biondi and Symes, 2003) presents one method to take advantage of this fact

to image all dips, using transformation to the angle domain. An alternative method works through image filtering, as follows.

Define a filter $\bar{\Psi}_z$ which annihilates the plane wave components of horizontal offset reflectivities \bar{R}_z with small k_z (relative to the other plane wave components). A precise definition of such a filter is given in Appendix D, and a cartoon in Figure ???. Then for any horizontal offset reflectivity \bar{R}_z , the filtered reflectivity $\bar{\Psi}_z \bar{R}_z$ does not contain vertically oriented reflectors, so that the relationship depicted in Figure ??? does not occur, and events in $\bar{F}[v]_z \bar{\Psi}_z \bar{R}_z$ are imaged only at zero offset.

Since the relation between event and reflector image location is the same with modeling and migration, this reasoning indicates that:

The quantitative versions of TIC and MSA, which are necessary for reliable imaging, imply that the filtered horizontal offset migration $R_z = \bar{\Psi}_z \bar{F}_z[v]^ d$ has (for correct migration velocity v) (i) energy at zero offset, and (ii) all other image energy confined to offsets at least h_{\min} .*

Note the contrast of this statement with the result obtained under the more restrictive DSR assumption: it is possible for the filtered migrated image volume to have energy at nonzero offset, even when the velocity is correct - this was impossible under DSR - but not inside the corridor $h < h_{\min}$.

R_z , computed as specified above, images reflectors with nonhorizontal dips. To fill out the dip range, one can adjoin the similarly computed vertical offset images

$$R_x = \bar{\Psi}_x \bar{F}_x[v]^* d, \quad R_y = \bar{\Psi}_y \bar{F}_y[v]^* d$$

The three volumes R_x, R_y, R_z together image all dips, and each has the local focussing property analogous to that already described for \bar{R}_z .

As noted in (Biondi and Symes, 2003), it is not possible to simply average the three volumes $\bar{R}_z, \bar{R}_y, \bar{R}_x$ to form a single image volume, when the velocity is not correct, due to a variation on the familiar phenomenon of image point dispersal. Of course when the velocity is correct, the versions of reflectors contained in the image volumes overlap, and can be added together to form a final image volume. [The filter definition explained in Appendix A is formulated to guarantee that this is possible, with no gaps and no artificially enhanced amplitudes.] However for velocity analysis (i.e. before a correct velocity has been achieved) these three volumes must be maintained as separate. See (Biondi and Symes, 2003) for a proposal to produce a single angle domain image volume which at least in some cases permits averaging the various image volumes (after Radon transform) even with incorrect velocity.

Two aspects of implementation should be noted immediately. It might be suspected that the production of three separate image volumes would be three times as expensive as the production of one image volume, but this is not the case. Most of the work (solution of the forward (1) and adjoint state (9) problems) is the same: these calculations must be performed once for each shot. Then the contribution for each shot is summed into the images according to equation (8) with the integration range of \mathbf{h} limited to

$(0, h_y, h_z)$, $(h_x, 0, h_z)$ and $(h_x, h_y, 0)$, and the corresponding filters $\bar{\Psi}_x$, $\bar{\Psi}_y$, and $\bar{\Psi}_z$ applied as postprocesses to produce \bar{R}_x , \bar{R}_y , and \bar{R}_z respectively.

Second, note that the filters $\bar{\Psi}_x$ etc. are truly *filters*, i.e. there is absolutely no need for spatial dependence. Therefore the filtering operation can be efficiently implemented in the Fourier domain.

EXAMPLES

The examples are all 2D (or will be, when they are done).

DISCUSSION

What is extent of the “corridor” around zero offset, how does this impact VA.

How can one enforce TIC and MSA without onerous ray tracing computations.

Acknowledgements

This work was supported in part by National Science Foundation grants DMS-9973423, DMS-9973308, and EAR-9977697, by the Los Alamos National Laboratory Computer Science Institute (LACSI) through LANL contract number 03891-99-23, ER14827, and by The Rice Inversion Project (TRIP). TRIP sponsors for 2002 were Amerada Hess Corp., Conoco Inc., Landmark Graphics Corp., Shell International Research, and Western Geco.

REFERENCES

- Biondi, B. and Shan, G. (2002). Prestack imaging of overturned reflections by reverse time migration. In *Expanded Abstracts, Society of Exploration Geophysicists, Annual International Meeting*, pages 1284–1287, Tulsa. SEG.
- Biondi, B. and Symes, W. (2003). Angle domain common-image gathers for migration velocity analysis. Technical report, Stanford Exploration Project, Stanford University.
- Chang, C. and McMechan, G. (1994). 3d elastic prestack reverse-time migration. *Geophysics*, 59.
- Claerbout, J. (1985). *Imaging the Earth’s Interior*. Blackwell Scientific Publishers, Oxford.
- Duistermaat, J. (1996). *Fourier Integral Operators*. Birkhauser, New York.
- Hormander, L. (1983). *The Analysis of Linear Partial Differential Operators*, volume I-IV. Springer Verlag, Berlin.
- Lailly, P. (1983). The seismic inverse problem as a sequence of before-stack migrations. In Bednar, J. et al., editors, *Conference on Inverse Scattering: Theory and Applications*, pages 206–220. SIAM, Philadelphia.

- Nolan, C. and Symes, W. (1997). Global solution of a linearized inverse problem for the wave equation. *Commun. in PDE*, 22(5&6):919–952.
- Nolan, C. J. and Symes, W. W. (1996). Imaging and conherency in complex structure. In *Expanded Abstracts, Society of Exploration Geophysicists, Annual International Meeting*, pages 359–363, Tulsa. SEG.
- Prucha, M., Biondi, B., and Symes, W. (1999). Angle-domain common-image gathers by wave equation migration. In *Expanded Abstracts, Society of Exploration Geophysicists, Annual International Meeting*, pages 824–827, Tulsa. SEG.
- Rakesh (1988). A linearized inverse problem for the wave equation. *Comm. on P.D.E.*, 13(5):573–601.
- Sava, P. and Fomel, S. (in press). Angle-domain common-image gahters by wavefield continuation methods. *Geophysics*.
- Stolk, C. (2000). *On the modeling and inversion of seismic data*. PhD thesis, Universiteit Utrecht.
- Stolk, C. ((in press)). Microlocal analysis of the scattering angle transform. *Comm. on P. D. E.*
- Stolk, C. and deHoop, M. (2001). Seismic inverse scattering in the 'wave-equation' approach. Technical report, Mathematical Sciences Research Institute, Berkeley, California, USA.
- Stolk, C. and Symes, W. (2002). Kinematic artifacts in prestack dpeth migration. Technical report, The Rice Inversion Project, Rice University.
- Tarantola, A. (1987). *Inverse Problem Theory*. Elsevier.
- Taylor, M. (1981). *Pseudodifferential Operators*. Princeton University Press, Princeton, New Jersey.
- tenKroode, A. P. E., Smit, D. J., and Verdel, A. R. (1998). A microlocal analysis of migration. *Wave Motion*, 28:149–172.
- Whitmore, D. (1983). Iterative depth migration by backward time propagation. In *Expanded Abstracts, Society of Exploration Geophysicists, Annual International Meeting*, Tulsa. SEG.
- Xu, S., Chauris, H., Lambaré, G., and Noble, M. (2001). Common angle migration: a strategy for imaging complex media. *Geophysics*, 66:1877–1894.
- Yoon, K., Shin, C., Suh, S., Lines, L., and Hong, S. (2003). 3d reverse-time migration using the acoustic wave equation: an experience with the seg/eage data set. *The Leading Edge*, 22:38–41.

APPENDIX A

This appendix gives a quick derivation of equation (8). For several examples of this type of computation, see (Tarantola, 1987)

The claim is that

$$F[v]^*d(\mathbf{x}, \mathbf{x}_h) = -\frac{2}{v(\mathbf{x})} \int dx_s \int_0^T dt \left(\frac{\partial q}{\partial t} \nabla^2 u \right) (\mathbf{x} - 2\mathbf{h}, t; \mathbf{x}_s)$$

where *adjoint field* q satisfies $q \equiv 0, t \geq T$ and

$$\left(\frac{1}{v^2} \frac{\partial^2}{\partial t^2} - \nabla^2 \right) q(\mathbf{x}, t; \mathbf{x}_s) = \int dx_r d(\mathbf{x}_r, t; \mathbf{x}_s) \delta(\mathbf{x} - \mathbf{x}_r)$$

To see this, form the standard inner products in the appropriate spaces (image on the left, data on the right):

$$\begin{aligned} & \langle F[v]^*d, r \rangle = \langle d, F[v]r \rangle \\ & = \int \int dx_s dx_r \int_0^T dt d(\mathbf{x}_r, t; \mathbf{x}_s) \frac{\partial u}{\partial t}(\mathbf{x}_r, t; \mathbf{x}_s) \\ & = \int dx_s \int dx \int_0^T dt \left\{ \int dx_r d(\mathbf{x}_r, t; \mathbf{x}_s) \delta(\mathbf{x} - \mathbf{x}_r) \right\} \frac{\partial \delta u}{\partial t}(\mathbf{x}, t; \mathbf{x}_s) \\ & = \int dx_s \int dx \int_0^T dt \left[\left(\frac{1}{v^2} \frac{\partial^2}{\partial t^2} - \nabla^2 \right) q \right] \frac{\partial \delta u}{\partial t}(\mathbf{x}, t; \mathbf{x}_s) \\ & = - \int dx_s \int dx \int_0^T dt \left[\left(\frac{1}{v^2} \frac{\partial^2}{\partial t^2} - \nabla^2 \right) \delta u \right] \frac{\partial q}{\partial t}(\mathbf{x}, t; \mathbf{x}_s) \end{aligned}$$

(boundary terms in integration by parts vanish because (i) $\delta u \equiv 0, t \ll 0$; (ii) $q \equiv 0, t \gg 0$; (iii) both vanish for large \mathbf{x} , at each t)

$$\begin{aligned} & = - \int dx_s \int dx \int_0^T dt \left(\frac{2r}{v^2} \frac{\partial^2 u}{\partial t^2} \frac{\partial q}{\partial t} \right) (\mathbf{x}, t; \mathbf{x}_s) \\ & = - \int dx_s \int dx r(\mathbf{x}) \frac{2}{v^2(\mathbf{x})} \int_0^T dt \left(\frac{\partial^2 u}{\partial t^2} \frac{\partial q}{\partial t} \right) (\mathbf{x}, t; \mathbf{x}_s) \\ & = \langle r, F[v]^*d \rangle \end{aligned}$$

q.e.d.

APPENDIX B

In this appendix we establish the relation between the appearance of events in the data and the presence of reflectors in the migrated image. This relation is the *same* for the forward modeling operator and for its adjoint, the migration operator.

The reasoning presented here shares with (Stolk and deHoop, 2001) the identification of events, respectively reflectors, by high frequency asymptotics in phase space, but differs in that it does not explicitly use the oscillatory integral representation of $F[v]$ derived in the last section. Instead, this argument follows the pattern of Rakesh's analysis of shot profile migration kinematics (Rakesh, 1988). It can be made mathematically rigorous, by means of the so-called Gabor calculus in the harmonic analysis of singularities (see (Duistermaat, 1996) Ch. 1).

The appearance of an event at a point $(\mathbf{x}_s, \mathbf{x}_r, t_{sr})$ in the data volume is equivalent to the presence of a sizeable Fourier coefficient for a plane wave component

$$e^{i\omega(t - \mathbf{p}_s \cdot \mathbf{y}_s - \mathbf{p}_r \cdot \mathbf{y}_r)}$$

in the acoustic field for frequencies ω within the bandwidth of the data, even after muting out all events at a small distance from $(\mathbf{x}_s, \mathbf{x}_r, t_{sr})$.

Note that the data does not necessarily fully determine this plane wave component, i.e. the full 3D event slownesses $\mathbf{p}_s, \mathbf{p}_r$. In this appendix, $\mathbf{p}_s, \mathbf{p}_r$ are assumed to be compatible with the data, in the sense just explained.

Assume that these frequencies are high enough relative to the length scales in the velocity that such local plane wave components propagate according to geometric acoustics. This assumption tacitly underlies much of reflection processing, and in particular is vital to the success of migration.

That is, solutions of wave equations such as (11) carry energy in local plane wave components along rays. Let $(\mathbf{X}_r(t), \mathbf{P}_r(t))$ denote such a ray, so that $\mathbf{X}_r(t_{sr}) = \mathbf{x}_r, \mathbf{P}_r(t_{sr}) = \mathbf{p}_r$. Then at some point the ray must pass through a point in phase space at which the source term (right hand side) of equation (11) has significant energy - otherwise the ray would never pick up any energy at all, and there would be no event at time t_{sr} , receiver position \mathbf{x}_r , and receiver slowness \mathbf{p}_r . [Supplemented with proper mathematical boilerplate, this statement is the celebrated *Propagation of Singularities* theorem of Hörmander, (Hörmander, 1983; Taylor, 1981).]

The source term involves (i) a product, and (ii) an integral in some of the variables. The Green's function $G(\mathbf{y}_s, t, \mathbf{x}_s)$ has high frequency components along rays from the source, i.e. at points of the form $(\mathbf{X}_s(t_s), \mathbf{P}_s(t_s))$ where $\mathbf{X}_s(0) = \mathbf{x}_s$ and $t_s \geq 0$. [Of course this is just another instance of Propagation of Singularities, as the source term in the wave equation for $G(\mathbf{y}_s, t_s, \mathbf{x}_s)$ is singular only at $(\mathbf{x}_s, 0)$.] That is, viewed as a function of \mathbf{y}_s and t_s , $G(\cdot, \cdot; \mathbf{x}_s)$ will have significant Fourier coefficients for plane waves

$$e^{i\omega(\mathbf{P}_s(t_s) \cdot \mathbf{y}_s + t_s)}$$

We characterize *reflectors* in the same way: that is, there is a (double) reflector at $(\mathbf{y}_s, \mathbf{y}_r)$ if \bar{R} has significant Fourier coefficients of a plane wave

$$e^{i(\mathbf{k}_s \cdot \mathbf{y}'_s + \mathbf{k}_r \cdot \mathbf{y}'_r)}$$

for some pair of wavenumbers $\mathbf{k}_s, \mathbf{k}_r$, and for generic points $(\mathbf{y}'_s, \mathbf{y}'_r)$ near $(\mathbf{y}_s, \mathbf{y}_r)$. Presumably then the product $R(\mathbf{y}'_s, \mathbf{x})G(\mathbf{y}'_s, t_s; \mathbf{x}_s)$ has a significant coefficient of the plane wave component

$$e^{i((\mathbf{k}_s + \omega \mathbf{P}_s(t_s)) \cdot \mathbf{y}'_s + \mathbf{k}_r \cdot \mathbf{x} + \omega t_s)}$$

for \mathbf{y}'_s near \mathbf{y}_s , \mathbf{x} near \mathbf{y}_r ; note that implicitly we have assumed that \mathbf{y}_s (the argument of G) is located on a ray from the source with time t_s . The right-hand side of equation (11) integrates this product over \mathbf{y}_s . This integral will be negligible unless the phase in \mathbf{y}_s is stationary: that is, to produce a substantial contribution to the RHS of equation (11), it is necessary that

$$\mathbf{y}_s = \mathbf{X}_s(t_s), \quad \mathbf{k}_s + \omega \mathbf{P}_s(t_s) = 0 \quad (20)$$

Supposing that this is so, the remaining exponential suggests that the RHS of equation (11) has a sizeable passband component of the form

$$e^{i(\mathbf{k}_r \cdot \mathbf{x} + \omega t_s)}$$

for \mathbf{x} near \mathbf{y}_r . As was argued above, this RHS will give rise to a significant plane wave component in the solution u arriving at \mathbf{x}_r at time $t_{sr} = t_s + t_r$ exactly when a ray arriving at \mathbf{x}_r at time t_{sr} starts from a position in space-time with the location and wavenumber of this plane wave, at time $t_s = t_{sr} - t_r$: that is,

$$\mathbf{X}_r(t_s) = \mathbf{y}_r, \quad \omega \mathbf{P}_r(t_s) = \mathbf{k}_r \quad (21)$$

We end this appendix with a remark about the case of *complete coverage*, i.e. sources and receivers densely sample a fully 2D area on or near the surface. Assuming that the effect of the free surface has been removed, so that all events may be viewed as samplings of an upcoming wavefield, the data (2D) event slowness uniquely determines the wavefield (3D) slowness through the eikonal equation. Thus an event in the data is characterized by its (3D) moveout: locally, by a moveout equation $t = T(\mathbf{x}_s, \mathbf{x}_r)$, and infinitesimally by the source and receiver slownesses

$$\mathbf{p}_s = \nabla_{\mathbf{x}_s} T, \quad \mathbf{p}_r = \nabla_{\mathbf{x}_r} T$$

In this case, the data event uniquely determines the source and receiver rays.

APPENDIX C

Start with zero-offset. Again, assume exploding reflector model:

$$\tilde{F}[v]r(\mathbf{x}_s, t) = w(\mathbf{x}_s, t), \quad \mathbf{x}_s \in X_s, \quad 0 \leq t \leq T$$

$$\left(\frac{4}{v^2} \frac{\partial^2}{\partial t^2} - \nabla^2 \right) w = \delta(t) \frac{2r}{v^2}, \quad w \equiv 0, \quad t < 0$$

Basic idea: 2nd order wave equation permits waves to move in all directions, but waves carrying reflected energy are (mostly) moving *up*. Should satisfy a 1st order equation for wave motion in one direction.

For the moment use 2D notation $\mathbf{x} = (x, z)$ etc. Write wave equation as evolution equation in z :

$$\frac{\partial^2 w}{\partial z^2} - \left(\frac{4}{v^2} \frac{\partial^2}{\partial t^2} - \frac{\partial^2}{\partial x^2} \right) w = -\delta(t) \frac{2r}{v^2}$$

Suppose that you could take the square root of the operator in parentheses - call it B . Then the LHS of the wave equation becomes

$$\left(\frac{\partial}{\partial z} - B \right) \left(\frac{\partial}{\partial z} + B \right) w = -\delta(t) \frac{2r}{v^2}$$

so setting

$$\tilde{w} = \left(\frac{\partial}{\partial z} + B \right) w$$

you get

$$\left(\frac{\partial}{\partial z} - B \right) \tilde{w} = -\delta(t) \frac{2r}{v^2}$$

which might be the required equation for upcoming waves.

Two major problems: (i) how the h-l do you take the square root of a PDO? (ii) what guarantees that the equation just written governs upcoming waves?

Calculus of pseudodifferential operators: recall that products of Ψ DOs are Ψ DOs. Computations simple for *subclass* of Ψ DOs with symbols given by asymptotic expansions:

$$p(\mathbf{x}, \xi) \sim \sum_{j \leq m} p_j(\mathbf{x}, \xi), \quad |\xi| \rightarrow \infty$$

in which p_j is *homogeneous in ξ of degree j* :

$$p_j(\mathbf{x}, \tau\xi) = \tau^j p_j(\mathbf{x}, \xi), \quad \tau, |\xi| \geq 1$$

The *principal symbol* is the homogeneous term of highest degree, i.e. p_m above.

Product rule for Ψ DOs: if

$$p^1(\mathbf{x}, \xi) = \sum_{j \leq m^1} p_j^1(\mathbf{x}, \xi), \quad p^2(\mathbf{x}, \xi) = \sum_{j \leq m^2} p_j^2(\mathbf{x}, \xi)$$

then principal symbol of $p^1(\mathbf{x}, D)p^2(\mathbf{x}, D)$ is $p_{m^1}^1(\mathbf{x}, \xi)p_{m^2}^2(\mathbf{x}, \xi)$, and there is an algorithm for computing the rest of the expansion.

In an open neighborhood $X \times \Xi$ of (\mathbf{x}_0, ξ_0) , symbol of $p^1(\mathbf{x}, D)p^2(\mathbf{x}, D)$ depends only on symbols of p^1, p^2 in $X \times \Xi$.

Consequence: if $a(\mathbf{x}, D)$ has an asymptotic expansion and is of order $m \in \mathbf{R}$, and $a_m(\mathbf{x}_0, \xi_0) > 0$ in $\mathcal{P} \subset \mathbf{R}^n \times \mathbf{R}^n - 0$, then there exists $b(\mathbf{x}, D)$ of order $m/2$ with asymptotic expansion for which

$$(a(\mathbf{x}, D) - b(\mathbf{x}, D)b(\mathbf{x}, D))u \in \mathcal{E}(\mathbf{R}^n)$$

for any $u \in \mathcal{E}'(\mathbf{R}^n)$ with $WF(u) \subset \mathcal{P}$.

Moreover, $b_{m/2}(\mathbf{x}, \xi) = \sqrt{a_m(\mathbf{x}, \xi)}$, $(\mathbf{x}, \xi) \in \mathcal{P}$. Will call b a *microlocal square root* of a .

Similar construction: if $a(\mathbf{x}, \xi) \neq 0$ in \mathcal{P} , then there is $c(\mathbf{x}, D)$ of order $-m$ so that

$$c(\mathbf{x}, D)a(\mathbf{x}, D)u - u, a(\mathbf{x}, D)c(\mathbf{x}, D)u - u \in \mathcal{E}(\mathbf{R}^n)$$

for any $u \in \mathcal{E}'(\mathbf{R}^n)$ with $WF(u) \subset \mathcal{P}$.

Moreover, $c_{-m}(\mathbf{x}, \xi) = 1/a_m(\mathbf{x}, \xi)$, $(\mathbf{x}, \xi) \in \mathcal{P}$. Will call c a *microlocal inverse* of a .

Application: symbol of

$$a(x, z, D_t, D_x) = \frac{\partial^2}{\partial x^2} - \frac{4}{v(x, z)^2} \frac{\partial^2}{\partial t^2} = \frac{4}{v(x, z)^2} D_t^2 - D_x^2$$

is

$$a(x, z, \tau, \xi) = \frac{4}{v(x, z)^2} \tau^2 - \xi^2$$

For $\delta > 0$, set

$$\mathcal{P}_\delta(z) = \left\{ (x, t, \xi, \tau) : \frac{4}{v(x, z)^2} \tau^2 > (1 + \delta) \xi^2 \right\}$$

Then according to the last slide, there is an order 1 Ψ DO-valued function of z , $b(x, z, D_t, D_x)$, with principal symbol

$$b_1(x, z, \tau, \xi) = \sqrt{\frac{4}{v(x, z)^2} \tau^2 - \xi^2} = \tau \sqrt{\frac{4}{v(x, z)^2} - \frac{\xi^2}{\tau^2}}, \quad (x, t, \xi, \tau) \in \mathcal{P}_\delta(z)$$

for which $a(x, z, D_t, D_x)u \simeq b(x, z, D_t, D_x)b(x, z, D_t, D_x)u$ if $WF(u) \subset \mathcal{P}_\delta(z)$.

b is the world-famous **single square root** (“SSR”) operator - see Claerbout, BEI.

To what extent has this construction factored the wave operator:

$$\begin{aligned} & \left(\frac{\partial}{\partial z} - ib(x, z, D_x, D_t) \right) \left(\frac{\partial}{\partial z} + ib(x, z, D_x, D_t) \right) \\ &= \frac{\partial^2}{\partial z^2} + b(x, z, D_x, D_t)b(x, z, D_x, D_t) + \frac{\partial b}{\partial z}(x, z, D_x, D_t) \end{aligned}$$

SSR Assumption: For some $\delta > 0$, the wavefield w satisfies

$$(x, z, t, \xi, \zeta, \tau) \in WF(w) \Rightarrow (x, t, \xi, \tau) \in \mathcal{P}_\delta(z) \text{ and } \zeta\tau > 0$$

This statement has a ray-theoretic interpretation (which will eventually make sense): rays carrying significant energy are nowhere horizontal. Along any such ray, z decreases as t increases - *coming up!*

$$\tilde{w}(x, z, t) = \left(\frac{\partial}{\partial z} + ib(x, z, D_x, D_t) \right) w(x, z, t)$$

$$b(x, z, D_x, D_t)b(x, z, D_x, D_t)w \simeq \left(\frac{4}{v(x, z)^2} D_t^2 - D_x^2 \right) w$$

with a smooth error, so

$$\begin{aligned} \left(\frac{\partial}{\partial z} - ib(x, z, D_x, D_t) \right) \tilde{w}(x, z, t) &= -\frac{2r(x, z)}{v(x, z)^2} \delta(t) \\ &+ i \left(\frac{\partial}{\partial z} b(x, z, D_x, D_t) \right) w(x, z, t) \end{aligned}$$

(since b depends on z , the z deriv. does not commute with b). So $\tilde{w} = \tilde{w}_0 + \tilde{w}_1$, where

$$\left(\frac{\partial}{\partial z} - ib(x, z, D_x, D_t) \right) \tilde{w}_0(x, z, t) = -\frac{2r(x, z)}{v(x, z)^2} \delta(t)$$

(this is the **SSR modeling equation**)

$$\left(\frac{\partial}{\partial z} - ib(x, z, D_x, D_t) \right) \tilde{w}_1(x, z, t) = i \left(\frac{\partial}{\partial z} b(x, z, D_x, D_t) \right) w(x, z, t)$$

Claim: $WF(\tilde{w}_1) \subset WF(w)$.

Granted this $\Rightarrow WF(\tilde{w}_0) \subset WF(w)$ also.

Upshot: SSR modeling

$$\tilde{F}_0[v]r(x_s, z_s, t) = \tilde{w}_0(x_s, z_s, t)$$

produces the same singularities (i.e. the same waves) as exploding reflector modeling, so is as good a basis for migration.

SSR migration: assume that sources all lie on $z_s = 0$.

$$\begin{aligned} &\langle \tilde{F}_0[v]^* d, r \rangle = \langle d, \tilde{F}_0[v] r \rangle \\ &= \int dx_s \int dt d(x_s, t) \tilde{w}_0(x_s, 0, t) \end{aligned}$$

$$= \int dx_s \int dt \int dz d(\bar{x}_s, t) \delta(z) \tilde{w}_0(x_s, z, t)$$

Define the adjoint field q by

$$\left(\frac{\partial}{\partial z} - b(x, z, D_x, D_t) \right) q(x, z, t) = d(x, t) \delta(z), \quad q(x, z, t) \equiv 0, \quad z < 0$$

which is equivalent to solving the initial value problem

$$\left(\frac{\partial}{\partial z} - ib(x, z, D_x, D_t) \right) q(x, z, t) = 0, \quad z > 0; \quad q(x, 0, t) = d(x, t)$$

Insert in expression for inner product, integrate by parts, use self-adjointness of b , get

$$\langle d, \tilde{F}_0[v]r \rangle = \int dx \int dz \frac{2r(x, z)}{v(x, z)^2} q(x, z, 0)$$

whence

$$\tilde{F}_0[v]^* d(x, z) = \frac{2}{v(x, z)^2} q(x, z, 0)$$

Standard description of this algorithm:

- downward continue data (i.e. solve for q)
- image at $t = 0$.

The art of SSR migration: computable approximations to $b(x, z, D_x, D_t)$ - swimming pool operator, many successors.

Unfinished business: proof of claim

Depends on celebrated **Propagation of Singularities** theorem of Hörmander (1970).

Given symbol $p(\mathbf{x}, \xi)$, order m , with asymptotic expansion, define *bicharacteristics* as solutions $(\mathbf{x}(t), \xi(t))$ of Hamiltonian system

$$\frac{d\mathbf{x}}{dt} = \frac{\partial p}{\partial \xi}(\mathbf{x}, \xi), \quad \frac{d\xi}{dt} = -\frac{\partial p}{\partial \mathbf{x}}(\mathbf{x}, \xi)$$

with $p(\mathbf{x}(t), \xi(t)) \equiv 0$.

Theorem: Suppose $p(\mathbf{x}, D)u = f$, and suppose that for $t_0 \leq t \leq t_1$, $(\mathbf{x}(t), \xi(t)) \notin WF(f)$. Then either $\{(\mathbf{x}(t), \xi(t)) : t_0 \leq t \leq t_1\} \subset WF(u)$ or $\{(\mathbf{x}(t), \xi(t)) : t_0 \leq t \leq t_1\} \subset T^*(\mathbf{R}^n) - WF(u)$.

At least two distinct proofs:

- Nirenberg, 1972

- Hörmander, 1970 (in Taylor, 1981)

Proof of claim: check that bicharacteristics for SSR operator are just upcoming rays of geom. optics for wave equation. These pass into $t < 0$ where RHS is smooth, also initial condn at large z is smooth - so each ray has one “end” outside of $WF(\tilde{w}_1)$. If ray carries singularity, must pass of WF of w , but then it’s entirely contained by P of S applied to w . **q. e. d.**

Nonzero offset (“prestack”): starting point is integral representation of the scattered field

$$F[v]r(\mathbf{x}_r, t; \mathbf{x}_s) = \frac{\partial^2}{\partial t^2} \int dx \frac{2r(\mathbf{x})}{v(\mathbf{x})^2} \int ds G(\mathbf{x}_r, t - s; \mathbf{x}) G(\mathbf{x}_s, s; \mathbf{x})$$

By analogy with zero offset case, would like to view this as “exploding reflectors in both directions”: reflectors propagate energy upward to sources and to receivers. However can’t do this because reflection location is *same* for both.

Bold stroke: introduce a new space variable \mathbf{y} , define

$$\tilde{F}[v]R(\mathbf{x}_r, t; \mathbf{x}_s) = \frac{\partial^2}{\partial t^2} \int \int dx dy R(\mathbf{x}, \mathbf{y}) \int ds G(\mathbf{x}_r, t - s; \mathbf{x}) G(\mathbf{x}_s, s; \mathbf{y})$$

and note that $\tilde{F}[v]R = F[v]r$ if

$$R(\mathbf{x}, \mathbf{y}) = \frac{2r}{v^2} \left(\frac{\mathbf{x} + \mathbf{y}}{2} \right) \delta(\mathbf{x} - \mathbf{y})$$

This trick decomposes $F[v]$ into two “exploding reflectors”:

$$\tilde{F}[v]R(\mathbf{x}_r, t; \mathbf{x}_s) = u(\mathbf{x}, t; \mathbf{x}_s)|_{\mathbf{x}=\mathbf{x}_r}$$

where

$$\begin{aligned} \left(\frac{1}{v(\mathbf{x})^2} \frac{\partial^2}{\partial t^2} - \nabla_{\mathbf{x}}^2 \right) u(\mathbf{x}, t; \mathbf{x}_s) &= \int dy R(\mathbf{x}, \mathbf{y}) G(\mathbf{x}_s, t; \mathbf{y}) \\ &\equiv w_s(\mathbf{x}_s, t; \mathbf{x}) \end{aligned}$$

(“upward continue the receivers”),

$$\left(\frac{1}{v(\mathbf{y})^2} \frac{\partial^2}{\partial t^2} - \nabla_{\mathbf{y}}^2 \right) w_s(\mathbf{y}, t; \mathbf{x}) = R(\mathbf{x}, \mathbf{y}) \delta(t)$$

(“upward continue the sources”).

This factorization of $F[v]$ ($r \mapsto R \mapsto \tilde{F}[v]R$) leads to a reverse time computation of adjoint with - will discuss on Friday.

It’s equally possible to continue the receivers first, then the sources, which leads to

$$\left(\frac{1}{v(\mathbf{y})^2} \frac{\partial^2}{\partial t^2} - \nabla_{\mathbf{y}}^2 \right) u(\mathbf{x}_r, t; \mathbf{y}) = \int dx R(\mathbf{x}, \mathbf{y}) G(\mathbf{x}_r, t; \mathbf{x})$$

$$\equiv w_r(\mathbf{x}_r, t; \mathbf{y})$$

(“upward continue the sources”),

$$\left(\frac{1}{v(\mathbf{x})^2} \frac{\partial^2}{\partial t^2} - \nabla_{\mathbf{x}}^2 \right) w_r(\mathbf{x}, t; \mathbf{y}) = R(\mathbf{x}, \mathbf{y}) \delta(t)$$

(“upward continue the receivers”).

Apply reverse depth concept: as before, go 2D temporarily, $\mathbf{x} = (x, z_r)$, $\mathbf{y} = (y, z_s)$, all sources and receivers on $z = 0$.

Double Square Root (“DSR”) assumption: For some $\delta > 0$, the wavefield u satisfies

$$(x, z_r, t, y, z_s, \xi, \zeta_s, \tau, \eta, \zeta_r) \in WF(u) \Rightarrow$$

$$(x, t, \xi, \tau) \in \mathcal{P}_\delta(z_r), (y, t, \eta, \tau) \in \mathcal{P}_\delta(z_s), \text{ and } \zeta_r \tau > 0, \zeta_s \tau > 0,$$

As for SSR, there is a ray-theoretic interpretation: rays from source and receiver to scattering point stay away from the vertical and decrease in z for increasing t , i.e. they are all upcoming.

Since z will be singled out (and eventually $R(\mathbf{x}, \mathbf{y})$ will have a factor of $\delta(\mathbf{x}, \mathbf{y})$), impose the constraint that

$$R(x, z, x, z_s) = \tilde{R}(x, y, z) \delta(z - z_s)$$

Define upcoming projections as for SSR:

$$\tilde{w}_s = \left(\frac{\partial}{\partial z_s} + ib(y, z_s, D_y, D_t) \right) w_s,$$

$$\tilde{w}_r = \left(\frac{\partial}{\partial z_r} + ib(x, z_r, D_x, D_t) \right) w_r,$$

$$\tilde{u} = \left(\frac{\partial}{\partial z_s} + ib(y, z_s, D_y, D_t) \right) \left(\frac{\partial}{\partial z_r} + ib(x, z_r, D_x, D_t) \right) u$$

Except for lower order commutators which we justify throwing away as before,

$$\left(\frac{\partial}{\partial z_s} - ib(y, z_s, D_y, D_t) \right) \tilde{w}_s = \tilde{R} \delta(z_r - z_s) \delta(t),$$

$$\left(\frac{\partial}{\partial z_r} - ib(x, z_r, D_x, D_t) \right) \tilde{w}_r = \tilde{R} \delta(z_r - z_s) \delta(t),$$

$$\left(\frac{\partial}{\partial z_r} - ib(x, z_r, D_x, D_t) \right) \tilde{u} = \tilde{w}_s$$

$$\left(\frac{\partial}{\partial z_s} - ib(y, z_s, D_y, D_t) \right) \tilde{u} = \tilde{w}_r$$

Initial (final) conditions are that \tilde{w}_r , \tilde{w}_s , and \tilde{u} all vanish for large z - the equations are to be solve in decreasing z (“upward continuation”).

Simultaneous upward continuation:

$$\begin{aligned} \frac{\partial}{\partial z} \tilde{u}(x, z, t; y, z) &= \frac{\partial}{\partial z_r} \tilde{u}(x, z_r, t; y, z)|_{z=z_r} + \frac{\partial}{\partial z_s} \tilde{u}(x, z, t; y, z_s)|_{z=z_s} \\ &= [ib(x, z_r, D_x, D_t) \tilde{u} + \tilde{w}_s + ib(y, z_s, D_y, D_t) \tilde{u} + \tilde{w}_r]_{z_r=z_s=z} \end{aligned}$$

Since $\tilde{w}_s(y, z, t; x, z) = \tilde{w}_r(x, z, t; y, z) = \tilde{R}(x, y, z)\delta(t)$, \tilde{u} is seen to satisfy the **DSR modeling equation**:

$$\left(\frac{\partial}{\partial z} - ib(x, z, D_x, D_t) - ib(y, z, D_y, D_t) \right) \tilde{u}(x, z, t; y, z) = 2\tilde{R}(x, y, z)\delta(t)$$

$$\tilde{F}[v] \tilde{R}(x_r, t; x_s) = \tilde{u}(x_r, 0, t; x_s, 0)$$

Computation of adjoint follows same pattern as for SSR, and leads to **DSR migration equation**: solve

$$\left(\frac{\partial}{\partial z} - ib(x, z, D_x, D_t) - ib(y, z, D_y, D_t) \right) \tilde{q}(x, y, z, t) = 0$$

in *increasing* z with initial condition at $z = 0$:

$$\tilde{q}(x_r, x_s, 0, t) = d(x_r, x_s, t)$$

Then $\tilde{F}[v]^* d(x, y, z) = \tilde{q}(x, y, z, 0)$

The physical DSR model has $\tilde{R}(x, y, z) = r(x, z)\delta(x - y)$, so final step in DSR computation of $F[v]^*$ is adjoint of $r \mapsto \tilde{R}$:

$$F[v]^* d(x, z) = \tilde{q}(x, x, z, 0)$$

Standard description of DSR migration (Claerbout, IEI):

- downward continue sources and receivers (solve DSR migration equation)
- image at $t = 0$ and zero offset ($x = y$)

Another moniker: “survey sinking”: DSR field \tilde{q} is (related to) the field that you would get by conducting the survey with sources and receivers at depth z . At any given depth, the zero-offset, time-zero part of the field is the instantaneous response to scatterers on which source = receiver is sitting, therefore constitutes an image.

As for SSR, the art of DSR migration is in the approximation of the DSR operator.

APPENDIX D

This appendix gives the mathematical details leading to the conclusion:

energy in a *properly filtered* source-receiver image volume is concentrated (i) at zero offset, and possibly (ii) at offsets greater than a minimum which depends on various characteristics of the velocity.

This conclusion depends on quantitative expressions of two conditions which are necessary for reliable imaging, as discussed in the section “Combining horizontal and vertical offsets”. The first of these is a quantitative version of the “maximum scattering angle”, or MSA, condition. This hypothesis was shown to be essential for imaging already in (Rakesh, 1988).

For any pair of rays $(\mathbf{X}_s, \mathbf{P}_s)$, $(\mathbf{X}_r, \mathbf{P}_r)$, the definition of the scattering angle θ is

$$\|v(\mathbf{X}_s)\mathbf{P}_s - v(\mathbf{X}_r)\mathbf{P}_r\|^2 = 2(1 + \cos\theta)$$

The quantitative MSA condition states that there is an angle $\theta_{\max} < \pi$ which is not exceeded by any ray pair carrying significant energy.

At a physical scattering point \mathbf{x} , where the rays meet, this means that

$$\|\mathbf{P}_s - \mathbf{P}_r\|^2 \geq 2(1 + \cos\theta_{\max})v^{-2}(\mathbf{x})$$

The second condition is a quantitative version of the Traveltime Injectivity Condition, or TIC, which was shown to be necessary in general for artifact-free imaging in (tenKroode et al., 1998). We assume that a constant $K > 0$ exists so that for any two rays $\mathbf{X}_s, \mathbf{X}_r$ meeting at time t_s ,

$$\|\mathbf{X}_s(t_s + \tau) - \mathbf{X}_r(t_s + \tau)\| \geq K \frac{|\tau|}{\sqrt{1 + \tau^2}} \quad (22)$$

That is, for small τ , points on the two rays at times $t_s + \tau$ are moving away from each other at rate K , and for large τ are asymptotically at least K apart.

In general, if source and receiver rays $(\mathbf{X}_s, \mathbf{P}_s)$, $(\mathbf{X}_r, \mathbf{P}_r)$ produce an image point for \bar{F}_z (i.e. with $\mathbf{X}_{s,z}(t_s) = \mathbf{X}_{r,z}(t_s)$) then we inherit a trajectory of imaging points for the unrestricted shot-geophone migration operator

$$\tau \rightarrow (\mathbf{X}_s(t_s + \tau), \mathbf{X}_r(t_s + \tau))$$

One of these is an image point for \bar{F}_z if $\mathbf{X}_{s,z}(t_s + \tau) = \mathbf{X}_{r,z}(t_s - \tau)$. From the ray equations,

$$\frac{d}{d\tau}[\mathbf{X}_{s,z}(t_s + \tau) - \mathbf{X}_{r,z}(t_s + \tau)] = v^2(\mathbf{X}_s(t_s + \tau))\mathbf{P}_{s,z}(t_s + \tau) - v^2(\mathbf{X}_r(t_s + \tau))\mathbf{P}_{s,z}(t_s + \tau)$$

Suppose that the velocity is correct, so that the rays image at zero offset: $\mathbf{X}_s(t_s) = \mathbf{X}_r(t_s) = \mathbf{x}$. Then

$$\frac{d}{d\tau}[\mathbf{X}_{s,z}(t_s + \tau) - \mathbf{X}_{r,z}(t_s + \tau)]_{\tau=0} = v^2(\mathbf{x}) \frac{k_z}{\omega}$$

From the slowness part of the ray equations, it follows that

$$\left\| \frac{d}{d\tau} v^{-2}(\mathbf{X}_a(t_s + \tau)) \frac{d}{d\tau} [\mathbf{X}_a(t_s + \tau)] \right\| \leq L,$$

in which a is either s or r and L is a global bound for $\|\nabla \log v\|$. From this it is easy to deduce that another global constant $M > 0$ exists, depending on L and on the max and min values of v , so that

$$\left| \frac{d^2}{d\tau^2} [\mathbf{X}_{s,z}(t_s + \tau) - \mathbf{X}_{r,z}(t_s + \tau)] \right| \leq M$$

for all τ . Thus the smallest nonzero value of τ for which

$$\mathbf{X}_{s,z}(t_s + \tau) - \mathbf{X}_{r,z}(t_s + \tau) = 0$$

has size proportional to k_z :

$$|\tau| \geq \frac{2}{M} v^2(\mathbf{x}) \left| \frac{k_z}{\omega} \right| \quad (23)$$

The foregoing suggests that as $k_z \rightarrow 0$, i.e. as reflector dip approaches vertical, then other points with arbitrarily small timeshift may image under application of \bar{F}_z , and indeed this is the case. Even worse from the point of view of velocity analysis, focussing at $h_x, h_y = 0$ is lost: according to quantitative TIC (equation (22)), one would expect that the imaging offset would vanish along with the time perturbation τ .

For a horizontal offset reflectivity of the form $R_z(x_s, y_s, x_r, y_r, z)$, define E_z to be the operator, already introduced, which produces a source-receiver reflectivity function:

$$E_z R_z(\mathbf{y}_s, \mathbf{y}_r) = r \left(x_s, y_s, x_r, y_r, \frac{z_s + z_r}{2} \right) \delta(z_s - z_r)$$

Define E_x and E_y similarly. If R is a physical reflectivity, i.e. $R(\mathbf{y}_s, \mathbf{y}_r) = r((\mathbf{y}_s + \mathbf{y}_r)/2) \delta(\mathbf{y}_s - \mathbf{y}_r)$, then there are restricted offset reflectivities R_x, R_y , and R_z for which $R = E_x R_x = E_y R_y = E_z R_z$, eg. $R_x(x, y_s, z_s, y_r, z_r) = r(x, (y_s + y_r)/2, (z_s + z_r)/2) \delta(y_s - y_r) \delta(z_s - z_r)$. That is, a physical reflectivity can be represented as the output of any of the three operators E_x, E_y, E_z .

Pick a number $\alpha > 1$. In Appendix D we show how to construct a triple of spatial filter operators Ψ_x, Ψ_y, Ψ_z so that

•

$$\Psi_x(\mathbf{k}_s, \mathbf{k}_r) + \Psi_y(\mathbf{k}_s, \mathbf{k}_r) + \Psi_z(\mathbf{k}_s, \mathbf{k}_r) \equiv 1$$

for all $(\mathbf{k}_s, \mathbf{k}_r)$;

•

$$\Psi_x(\mathbf{k}_s, \mathbf{k}_r) = 0 \text{ if } |k_{s,x} + k_{r,x}| < \alpha^{-1} \sqrt{|k_{s,x} + k_{r,x}|^2 + |k_{s,z} + k_{r,z}|^2}$$

$$\Psi_x(\mathbf{k}_s, \mathbf{k}_r) = 1 \text{ if } |k_{s,x} + k_{r,x}| > \alpha \sqrt{|k_{s,x} + k_{r,x}|^2 + |k_{s,z} + k_{r,z}|^2}$$

and similarly for Ψ_y, Ψ_z .

If the reflector wavenumber $(\mathbf{k}_s, \mathbf{k}_r)$ is such that $\Psi_z(\mathbf{k}_s, \mathbf{k}_r) > 0$, then from the defining properties of Ψ_z it follows that

$$\begin{aligned} (1 + \alpha^2) \frac{|k_{s,z} + k_{r,z}|^2}{\omega^2} &\geq \frac{\|\mathbf{k}_s + \mathbf{k}_r\|^2}{\omega^2} = \|\mathbf{P}_s - \mathbf{P}_r\|^2 \\ &\geq 2(1 + \cos \theta_{\max})v^{-2}(\mathbf{x}) \end{aligned} \quad (24)$$

Introduce filters $\bar{\Psi}_x$, $\bar{\Psi}_y$, and $\bar{\Psi}_z$ on restricted offset reflectivities, defined by the relation

$$\bar{\Psi}_x E_x = E_x \bar{\Psi}_x \quad (25)$$

and similarly for $\bar{\Psi}_y$ and $\bar{\Psi}_z$. These filters have the properties

$$\bar{\Psi}_z(k_{s,x}, k_{s,y}, k_{r,x}, k_{r,y}, k_z) = 0 \text{ if } |k_z| < \alpha^{-1} \sqrt{|k_{s,x} + k_{r,x}|^2 + |k_{s,y} + k_{r,y}|^2}$$

$$\bar{\Psi}_z(k_{s,x}, k_{s,y}, k_{r,x}, k_{r,y}, k_z) = 1 \text{ if } |k_z| > \alpha \sqrt{|k_{s,x} + k_{r,x}|^2 + |k_{s,y} + k_{r,y}|^2}$$

and similarly for $\bar{\Psi}_x$, $\bar{\Psi}_y$.

Now suppose that horizontal offset reflectivity R_z contains a physical reflectivity

$$R_z(x_s, y_s, x_r, y_r, z) = r(x, y, z) \delta\left(x - \frac{x_s + x_r}{2}\right) \delta\left(y - \frac{y_s + y_r}{2}\right) + \dots$$

and that there is a significant component with of the physical reflectivity with vertical wavenumber k_z after filtering by $\bar{\Psi}_z$. That is, for rays $(\mathbf{X}_s, \mathbf{P}_s)$, $(\mathbf{X}_r, \mathbf{P}_r)$ and scattering time t_s , the rays intersect at \mathbf{x} with the scatterer wavenumber $\omega(\mathbf{P}_r(t_s) - \mathbf{P}_s(t_s))$ having z component k_z . From relations (25, 24) it follows that

$$\frac{k_z^2}{\omega^2} \geq \frac{2(1 + \cos \theta_{\max})}{(1 + \alpha^2)} v^2(\mathbf{x}) \quad (26)$$

From inequalities (26, 23), it follows that any other point on these two rays which are imaged in $\bar{\Psi}_z R_z$, i.e. at which $\mathbf{X}_{s,z}(t_s + \tau) = \mathbf{X}_{r,z}(t_s + \tau)$ for some τ , requires that

$$|\tau| \geq \frac{2v(\mathbf{x})}{M} \sqrt{\frac{2(1 + \cos \theta_{\max})}{(1 + \alpha^2)}} \quad (27)$$

The relations (27, 22) therefore imply that any such secondary image point must occur at an offset $(h_x, h_y) = (\mathbf{X}_{s,x}(t_s + \tau) - \mathbf{X}_{r,x}(t_s + \tau), \mathbf{X}_{s,y}(t_s + \tau) - \mathbf{X}_{y,x}(t_s + \tau))$ satisfying

$$h^2 \equiv h_x^2 + h_y^2 \geq h_{\min}^2 \quad (28)$$

in which h_{\min} depends on max and min values of velocity and velocity gradient length, θ_{\max} , the TIC constant K , and the filter aperture α .

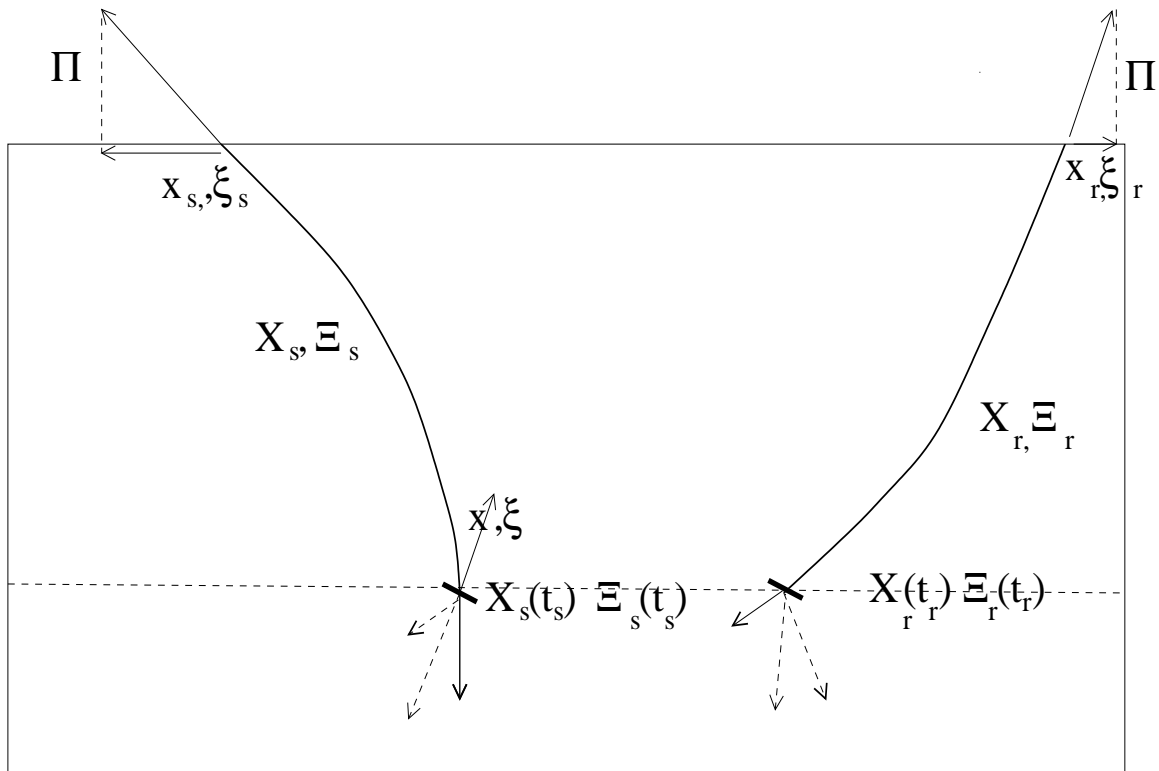


FIG. 1. Ray theoretic relation between data event and double reflector.

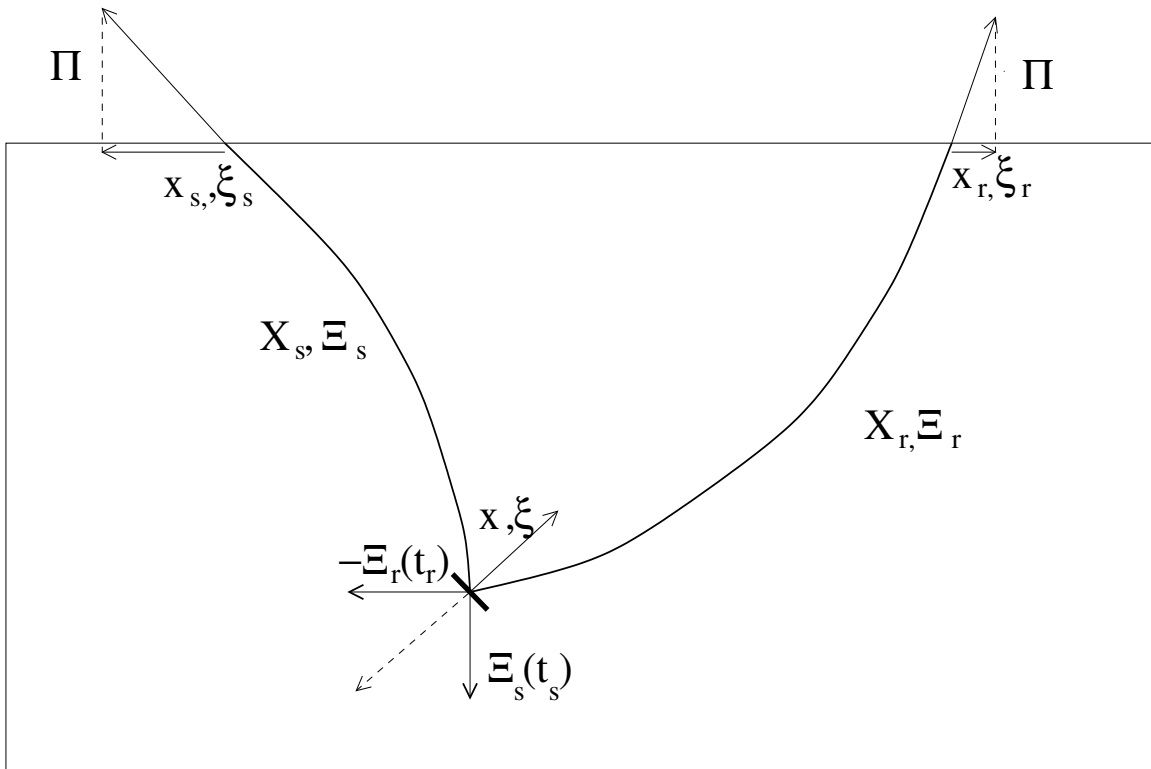


FIG. 2. Ray theoretic relation between data event and physical (single) reflector.

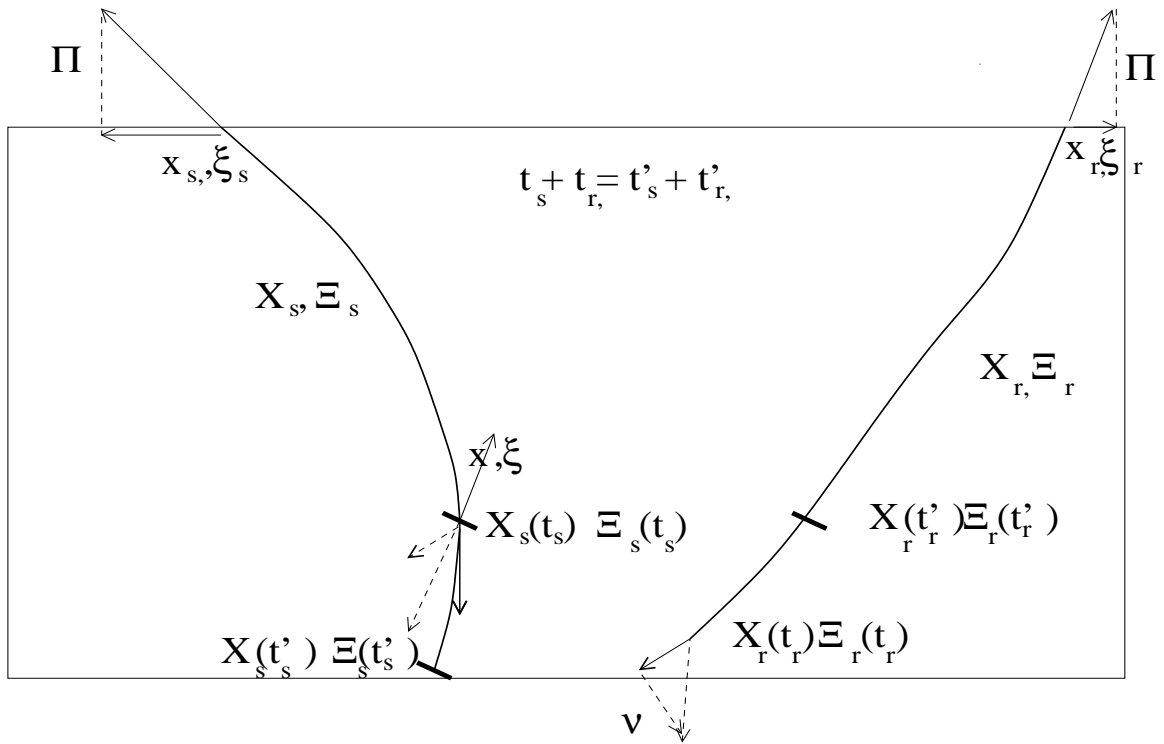


FIG. 3. Ambiguity of event-reflector relation: only total travelttime is constrained.

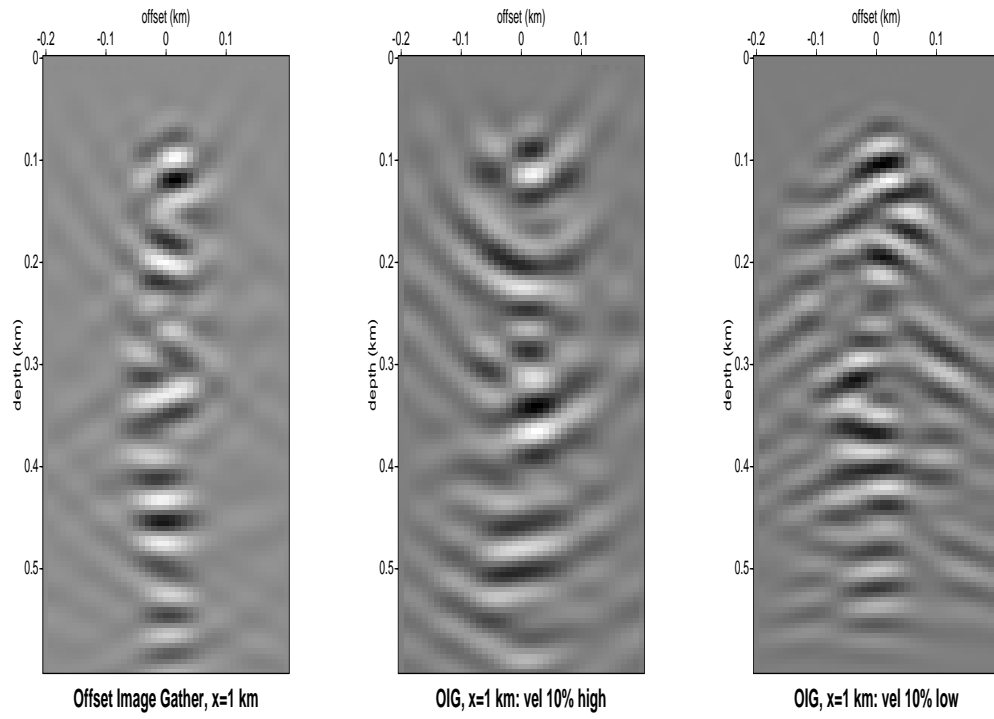


FIG. 4. Image gathers of data from random reflectivity, from left to right: correct velocity, 10% high, 10% low

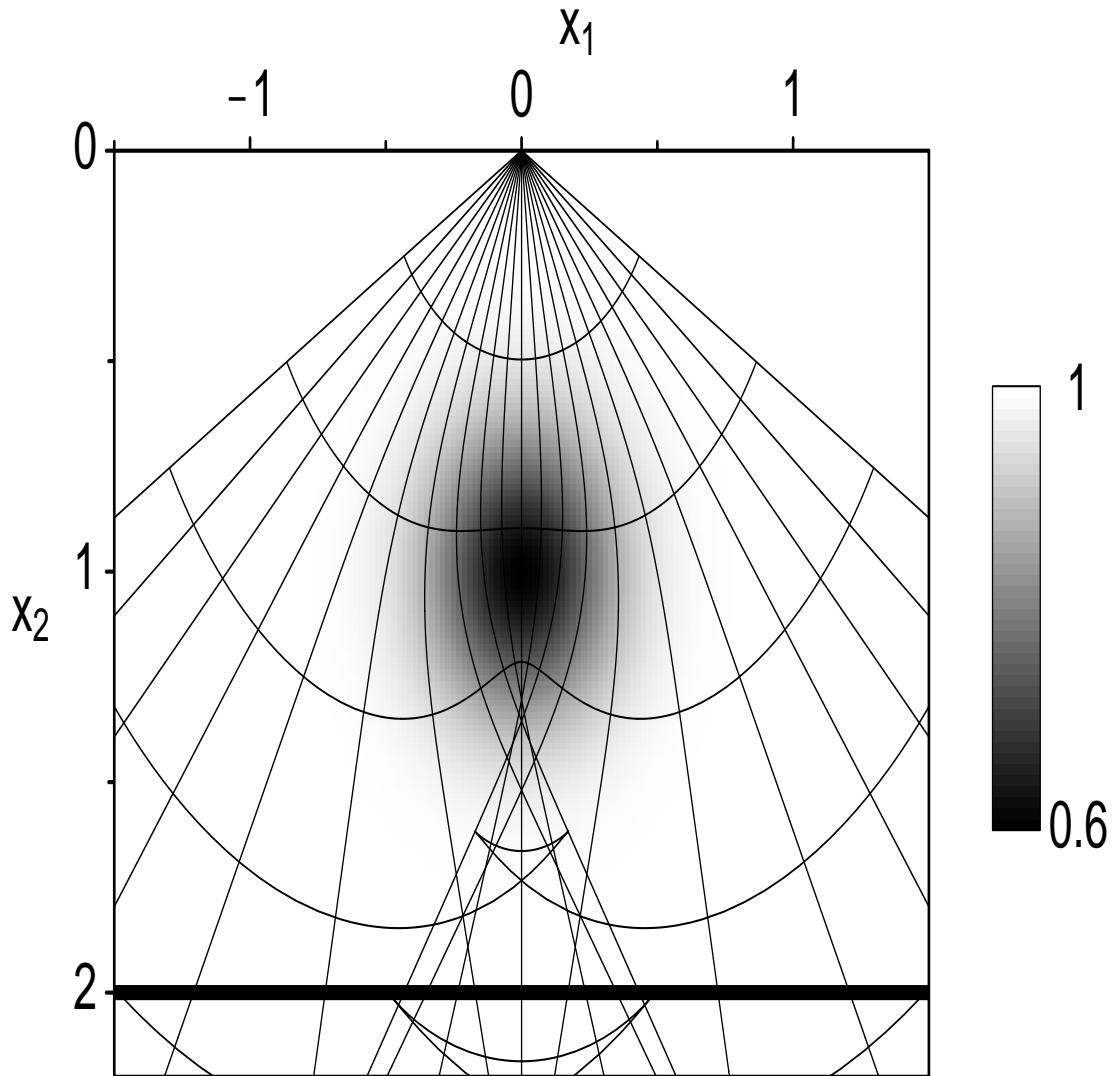


FIG. 5. Lens velocity model, reflector, and modest-offset rays.

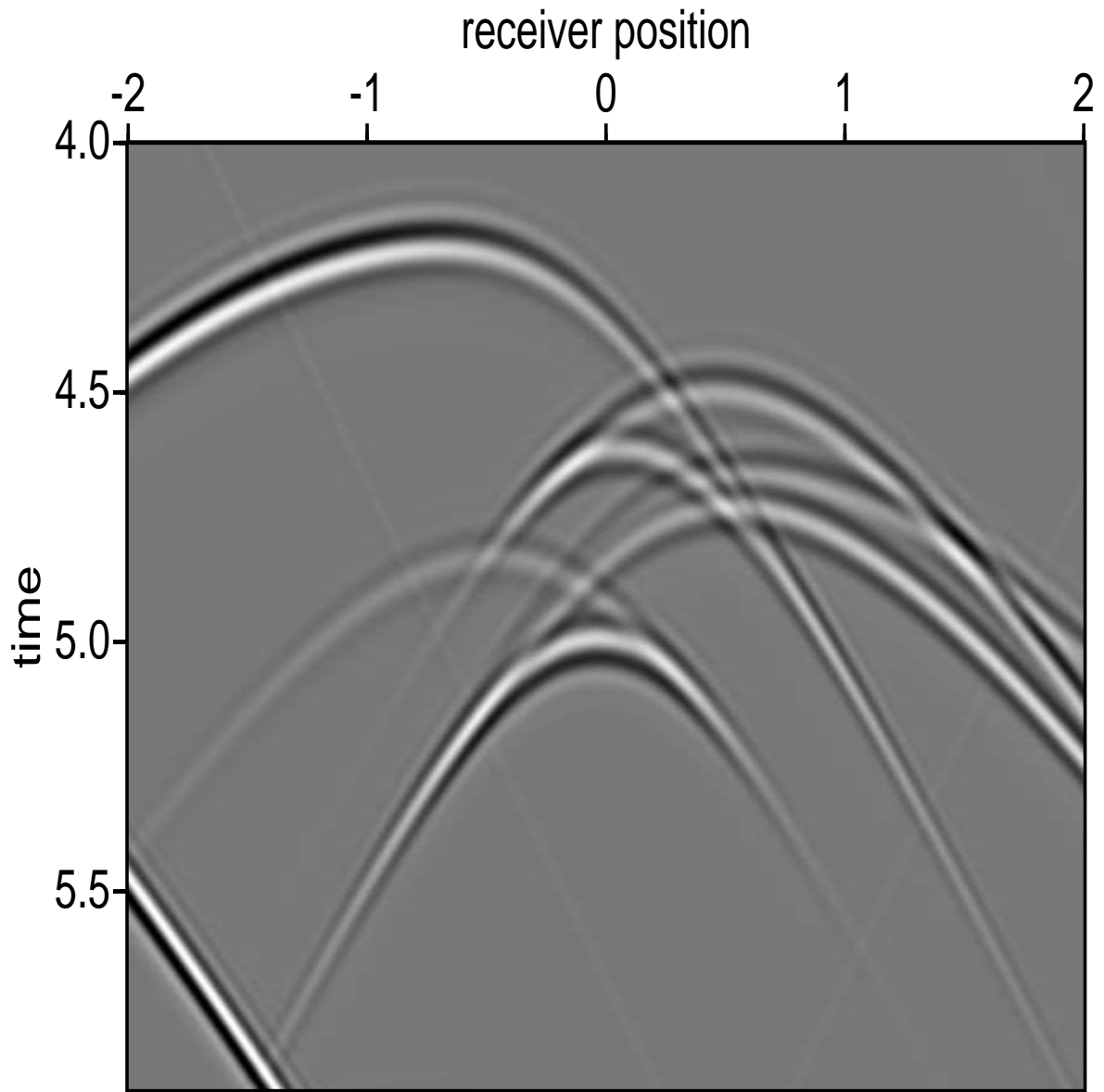


FIG. 6. Lens model: shot record, offset -0.5 km

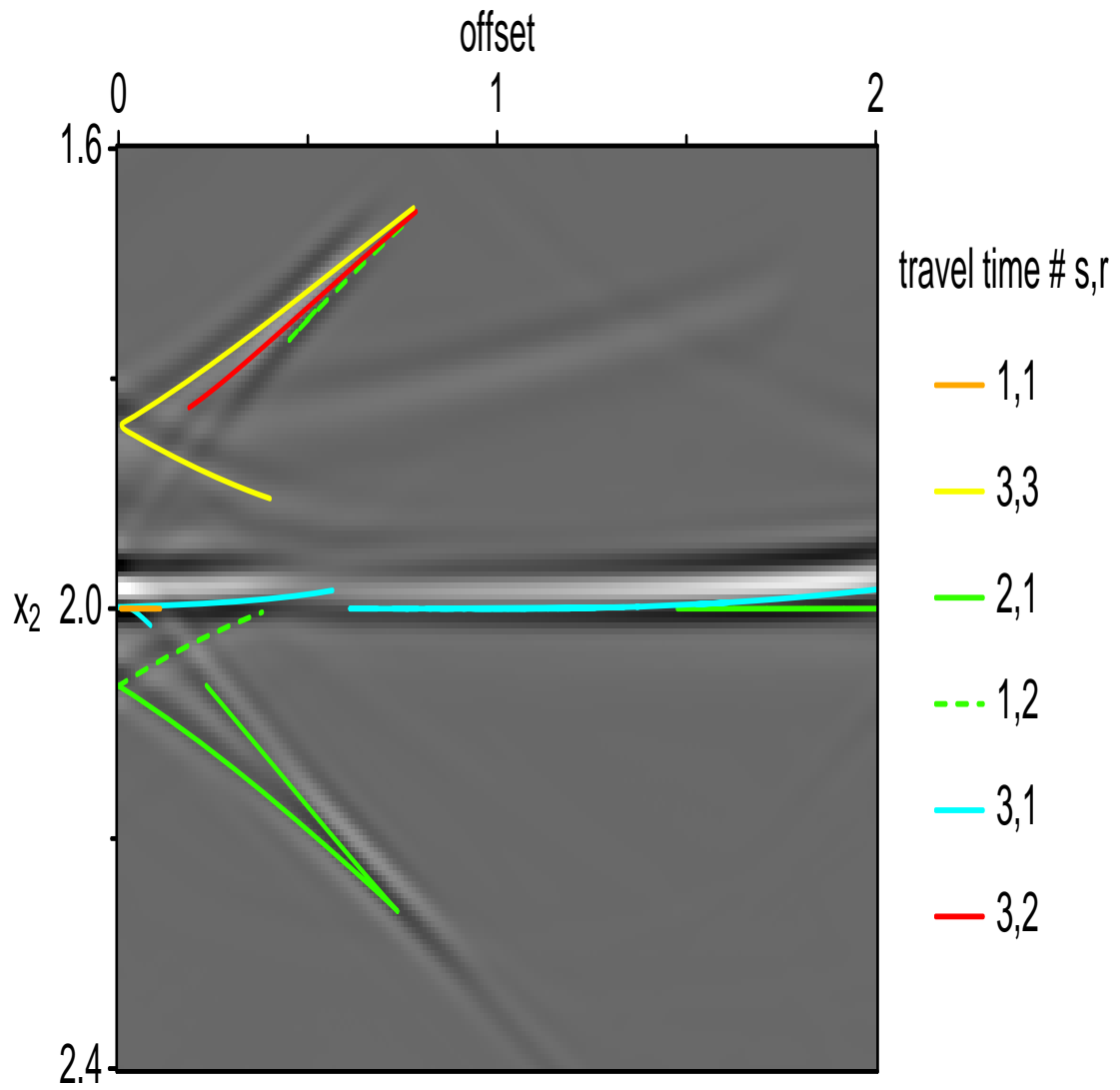


FIG. 7. Lens model: Kirchhoff common offset image gather, $x = 0.3$ km.

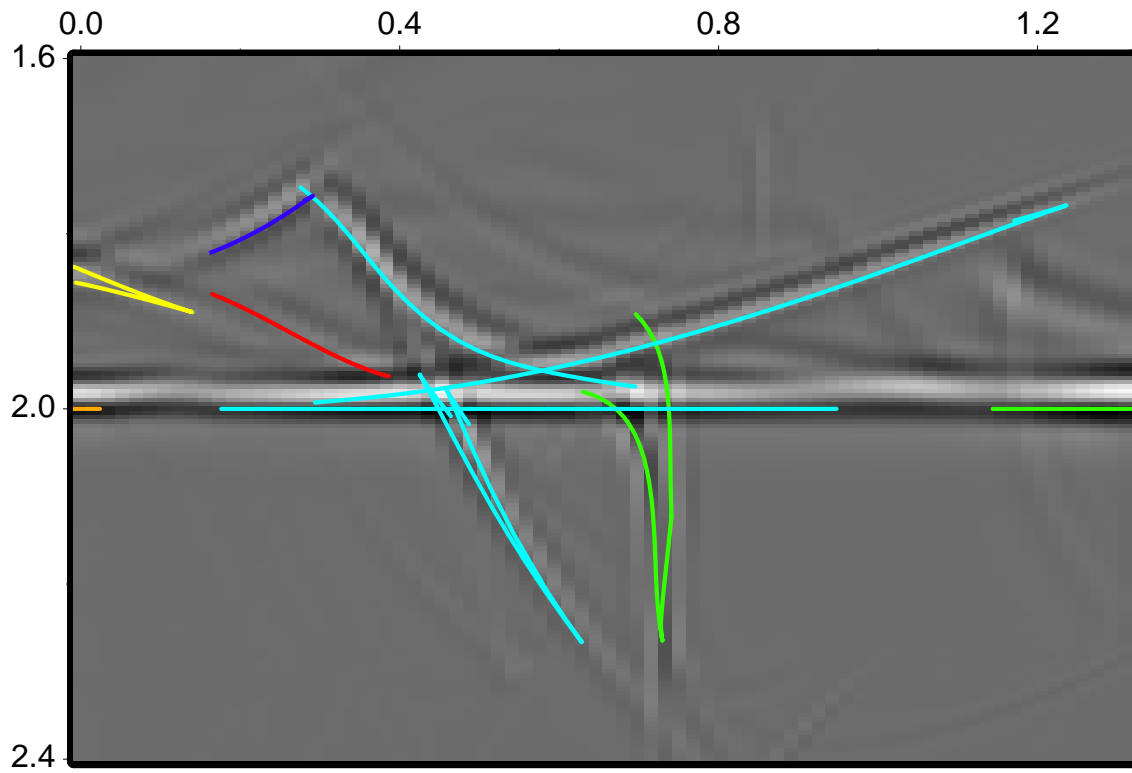


FIG. 8. Lens model: Kirchhoff common scattering angle image gather, $x = 0.3$ km.